

EE-LLM: Large-Scale Training and Inference of Early-Exit Large Language Models with 3D Parallelism

Yanxi Chen*, Xuchen Pan*, Yaliang Li[†], Bolin Ding, Jingren Zhou
 {chenyanxi.cyx, panxuchen.pxc, yaliang.li, bolin.ding, jingren.zhou}@alibaba-inc.com
 Alibaba Group

Abstract

We present EE-LLM, a framework for large-scale training and inference of early-exit large language models (LLMs). While recent works have shown preliminary evidence for the efficacy of early exiting in accelerating LLM inference, EE-LLM makes a foundational step towards scaling up early-exit LLMs by supporting their training and inference with massive 3D parallelism. Built upon Megatron-LM, EE-LLM implements a variety of algorithmic innovations and performance optimizations tailored to early exiting, including a lightweight method that facilitates backpropagation for the early-exit training objective with pipeline parallelism, techniques of leveraging idle resources in the original pipeline schedule for computation related to early-exit layers, and two approaches of early-exit inference that are compatible with KV caching for autoregressive generation. Our analytical and empirical study shows that EE-LLM achieves great training efficiency with negligible computational overhead compared to standard LLM training, as well as outstanding inference speedup without compromising output quality. To facilitate further research and adoption, we release EE-LLM at <https://github.com/pan-x-c/EE-LLM>.¹

Contents

1	Introduction	2
1.1	Goal and motivations	2
1.2	Challenges	3
1.3	Main contributions	3
2	Preliminaries	3
2.1	Transformers	3
2.2	Early-exit LLMs	4
2.3	Megatron-LM and 3D parallelism	4
3	An overview of EE-LLM	5
3.1	Model architectures	5
3.2	Training	5
3.3	Inference	5
4	Training	6
4.1	Backpropagation through pipeline stages	6
4.2	Training efficiency	8
4.3	Advanced features	11
5	Inference	13
5.1	Main challenge: KV caching	13
5.2	A new solution: pipeline parallelism	14

*Co-first authors.

[†]Corresponding author.

¹We will continuously update the codebase and arXiv version.

6	Implementations	14
6.1	Model architectures	14
6.2	Pipeline scheduling	15
6.3	Inference service	15
7	Experiments	15
7.1	Training	15
7.2	Inference	16
8	Related works	21
9	Conclusions	21
A	Analysis of training efficiency	22
A.1	Training time per iteration	22
A.2	Peak GPU memory	23
B	Supplementary materials for Section 4.3.2	24
B.1	Methodology	24
B.2	Analysis	25

1 Introduction

Large language models (LLMs) have amazed the world with their astonishing abilities and performance in solving a wide range of problems [8, 50, 11, 89, 74, 75]. This is accompanied by excessive costs and carbon emissions for training and deploying these models, as their sizes grow rapidly in recent years. In general, costs for inference are dominant in the long run, as each model will be deployed to solve many problems for a long period of time. This has inspired researchers and engineers to develop various approaches for accelerating LLM inference.

The focus of this work is *early exiting*, which accelerates inference by allowing a deep neural network to make predictions and exit early in the network for certain inputs, without running the forward pass through the full network. This is achieved by augmenting a standard neural network architecture (with a single exit at the end) with additional early-exit layers that transform intermediate hidden states into early outputs. The early-exit model architecture, as visualized in Figure 1, not only retains the full capacity of a large model, but is also capable of adaptively using a smaller amount of computation for solving simpler problems. The idea of early exiting is a natural analogue of how human speaks, thinks, and make decisions: not every problem requires or deserves the same amount of consideration, and one shall opt for fast reaction to simple problems without overthinking [31]. Early exiting has been an active research area and widely applied in natural language processing, computer vision, and other areas [23, 45, 25, 94, 19, 63, 81, 62, 82, 42, 26, 73, 27, 31, 38, 60, 24, 83, 14]. More recently, it starts to gain attention in the LLM domain [62, 13, 3, 76], and is recognized as a promising direction for further reducing the latency and costs of LLM inference [53].

1.1 Goal and motivations

The primary goal of this work is to build the infrastructure for *scaling up* training and inference of early-exit LLMs. This is motivated by the observation that the sizes of early-exit models in prior works are still relatively small. The largest early-exit LLM that we are aware of is a Llama 2 model [75] with 13 billion (13B) parameters [76]; in contrast, standard LLMs at much larger scales, e.g. the 175B GPT-3 [8], 530B Megatron-Turing NLG [68], 540B PaLM [11], or even larger sparsely activated models, have been well trained and deployed in many applications. It is an urgent need for the community to truly understand the efficacy of early exiting for LLMs at larger scales, which is indispensable for making early exiting a useful and practical option in complex scenarios that only sufficiently large LLMs can handle.

1.2 Challenges

The first and foremost question is how to train an early-exit LLM that is too large to fit into the memory of one single device (e.g. GPU). While state-of-the-art frameworks like Megatron-LM [67, 49, 36], DeepSpeed [58, 68], Mesh-TensorFlow [65], Alpa [92], InternLM [72], and many more, support training standard LLMs at large scales with data parallelism and model parallelism (including tensor, sequence and pipeline parallelism), they do not provide native support for early-exit LLMs. One particular challenge lies in pipeline parallelism [47, 48, 20, 41], which partitions the model along the depth dimension into multiple pipeline stages, connected by limited point-to-point communication between devices; this seems to contradict with early-exit models, as the early-exit training loss is typically an aggregation of losses for multiple (early or final) exits that are now located separately on different pipeline stages. Despite the necessity of pipeline parallelism in many scenarios, we are not aware of any implementation that supports training early-exit LLMs with pipeline parallelism.

Moreover, training efficiency for early-exit LLMs requires special design. While sizes of early-exit layers are often regarded as negligible for many neural network architectures, this is not the case for LLMs, where each early exit contains (at least) a large output embedding matrix that transforms hidden states into logits on the vocabulary. A naive implementation of early-exit LLM training can cause large computational overhead compared to standard LLM training.

Finally, with regards to autoregressive generation tasks (where tokens are generated one by one, depending on previously generated tokens via the attention mechanism), a naive implementation of early-exit inference is not compatible with KV caching, a standard technique of storing the keys and values of previously generated tokens at each layer. More specifically, if the current token is generated via early exiting at some layer, then its KV caches in later layers are missing, which hinders the generation of future tokens. Given that KV caching is enabled by default in most cases, the efficacy of early exiting for autoregressive generation might be questionable if its conflict with KV caching is not well resolved.

1.3 Main contributions

We propose **EE-LLM**, a system for large-scale training and inference of early-exit (EE) LLMs with 3D parallelism, which is designed to tackle the aforementioned challenges. **EE-LLM** is built upon Megatron-LM [67, 49, 36, 68], and augments it with various functionalities for early exiting. In addition to compatibility with existing functionalities of 3D parallelism provided by Megatron-LM, **EE-LLM** also implements a variety of algorithmic innovations, including a lightweight method that facilitates backpropagation for the early-exit training objective through pipeline stages, various techniques of leveraging idle resources in the original pipeline schedule for computation related to early-exit layers, and two approaches of early-exit inference that are compatible with KV caching (with one based on a novel form of pipeline parallelism and another based on KV recomputation). Implementation of **EE-LLM** has been well optimized for maximum training and inference efficiency. Our analytical and empirical study confirms that, with negligible computational overhead (caused by early-exit layers) during training with 3D parallelism, one obtains an early-exit LLM that generates tokens with adaptive token-wise exit selection, achieving outstanding speedup without compromising output quality during inference. In other words, **EE-LLM** facilitates training and inference of early-exit LLMs that are as large as the maximum sizes of standard LLMs allowed by Megatron-LM, given the same amount of computational resources. The source code for **EE-LLM** can be found at <https://github.com/pan-x-c/EE-LLM>.

2 Preliminaries

2.1 Transformers

The Transformer architecture [77, 71] has been playing a dominant role in natural language processing (NLP) and large language models (LLMs) [7, 90]. It is typically composed of an input embedding layer, a stack of Transformer layers, and finally an output layer. Each Transformer layer consists of cross-attention and/or self-attention modules [4, 34, 52], a multi-layer perceptron (MLP), and layer normalization (LayerNorm [2] or RMSNorm [88]). Transformers can be categorized into three types: encoder-only, encoder-decoder, and decoder-only. For the latter two, there is an output embedding matrix in the output layer, which

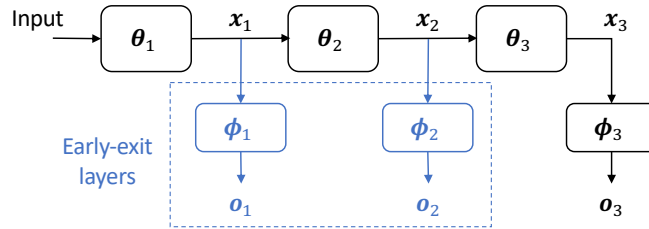


Figure 1: The model architecture of an early-exit LLM. New components related to early exiting, which are absent from a standard LLM, are highlighted in blue color. In this figure, each θ_i represents a sequence of Transformer layers in the backbone of the LLM (with some additional modules in θ_1 for input processing); in addition, each ϕ_i represents an early-exit or final-output layer that converts the hidden state x_i into an output o_i , e.g. logits for next-token prediction.

transforms hidden states into logits on a (typically large) vocabulary that can be used for generating tokens. An LLM can be learned by unsupervised pre-training, e.g. minimizing the negative log-likelihood of next-token prediction on a large corpus [55, 56]. In this work, we focus on the decoder-only generative pre-training (GPT) Transformer architecture [55, 56], though many of our ideas are widely applicable to other Transformer architectures or generic deep neural networks.

2.2 Early-exit LLMs

As mentioned earlier, an early-exit neural network can be obtained by adding to a standard neural network some early-exit layers that turn intermediate hidden states into early outputs [81, 63]. During inference for a given input, the model starts a forward pass and decides (at each early exit) whether to return an output or continue forwarding via certain rules, e.g. to return an output whenever the confidence of prediction is above a pre-defined threshold [63, 61].

The standard way of training an early-exit model is to minimize a weighted sum of early-exit and final-exit training losses [63, 61]. Note that early-exit layers bring additional computational overhead to training. This is especially the case for LLMs, primarily due to the large output embedding matrix of size $h \times V$ within each early-exit layer, where h is the hidden dimension and V is the vocabulary size. We call an early-exit layer *minimalistic* if it has the same structure as the final output layer of the GPT model architecture [55, 56], which includes an output embedding matrix, plus an optional LayerNorm/RMSNorm in front of it. Additional modules can be added to early-exit layers for increased expressivity and adaptivity of early exits.

2.3 Megatron-LM and 3D parallelism

Megatron-LM [67, 49, 36, 68] is one of the state-of-the-art systems for large-scale training of LLMs with 3D parallelism on a massive number of GPUs. With *data parallelism*, each GPU handles the forward and backward computation for one part of the data batch, and then the results are aggregated at the end of the training iteration. When the model is too large to fit in a single GPU, model partitioning becomes necessary and can be used in conjunction with data parallelism. With *tensor (and sequence) parallelism*, each large module (e.g. a linear layer) is divided into multiple pieces that are assigned to different GPUs, so that each computational task related to it (e.g. large matrix multiplication) can be divided into smaller tasks and solved in parallel. One major limitation with tensor (and sequence) parallelism is that it requires expensive collective communication such as all-reduce operations, and thus is only viable for high-end GPUs within the same computing node, with high-bandwidth communication among them.

Pipeline parallelism [47, 48, 20, 41], on the other hand, partitions a deep model along the depth dimension into multiple pipeline stages. Moreover, each data batch is divided into multiple microbatches, and their forward/backward computational tasks are scheduled among those multiple pipeline stages. More specifically, each stage performs the forward computation for each microbatch and sends the resulted hidden states to another stage; later on, it performs the backward computation for the same microbatch after receiving the gradients of the training objective with respect to the sent hidden states. Pipeline parallelism only

requires sparse and inexpensive point-to-point (P2P) communication between pipeline stages, which makes it applicable and oftentimes must-have in much broader scenarios when tensor (and sequence) parallelism is infeasible or insufficient, whether in GPU clusters or in decentralized settings [86, 84]. The main concern with pipeline parallelism is its low utilization rate of computational resources, due to pipeline bubbles and load imbalance across pipeline stages [49]; this will be discussed in more details in Section 4.2.

3 An overview of EE-LLM

This section provides an overview of our system for scaling up sizes, training and inference of early-exit LLMs, with flexible configurations and a wide range of functionalities. More details about training and inference will be introduced in Sections 4 and 5, respectively. Implementation details can be found in Section 6.

3.1 Model architectures

We implement in EE-LLM an early-exit Transformer architecture (which is built upon the GPT Transformer architecture [55, 56] originally implemented in Megatron-LM), with support for various configurations. In particular, users can (1) specify arbitrary layers to add early exits to; (2) add trainable modules to each early-exit layer (between the hidden states on the backbone and the minimalistic early-exit output head), such as an MLP or a complete Transformer layer; and (3) choose to tie [54, 61, 76] or untie the input and output embedding matrices of all early-exit/final-exit layers. Each particular configuration has its own pros and cons, as will be discussed in later sections. With this in mind, EE-LLM has been designed to cover a wide range of common configurations, so that users can easily try them out and choose the most suitable ones for their own use cases.

3.2 Training

EE-LLM contains the essential functionalities for training early-exit LLMs, which tackle the main challenges outlined in Section 1.2, i.e. how to train with 3D parallelism (especially pipeline parallelism) while minimizing the computational overhead (compared to standard LLM training) caused by early-exit layers. In addition to substantial engineering efforts for compatibility with existing functionalities in Megatron-LM, we design and implement a simple yet effective algorithm that facilitates pipeline parallelism with multiple early-exit or final-output training losses located on different pipeline stages, which is not possible in standard pipeline parallelism implemented by Megatron-LM or other frameworks. Moreover, our analytical and empirical study shows that training an early-exit LLM with EE-LLM is almost as efficient as training a standard LLM, in terms of training time and peak GPU memory; this is achieved by various performance optimizations that we design and implement in EE-LLM, especially the ones that passively or actively leverage idle computational resources in pipeline parallelism. Finally, EE-LLM contains some advanced features for more fine-grained control or optimization of the training procedure, including the option of changing early-exit loss weights during training, and a novel method of further improving resource utilization by filling pipeline bubbles with useful computation.

3.3 Inference

We design and implement two methods to tackle the major challenge of early-exit LLM inference for autoregressive generation, namely the conflict between early exiting and KV caching (as explained in Section 1.2). One method is based on KV recomputation, which runs the forward pass with a list of recent tokens when generating each token, and can be regarded as a variant of synchronized parallel decoding recently proposed in [3]. The other method is based on a novel form of pipeline parallelism, which parallelizes the forward pass of the current token at a certain pipeline stage with some KV-related computation (if any) of previous tokens at later stages.

4 Training

In this section, we first introduce (in Section 4.1) the essentials of scaling up early-exit LLM training with massive 3D parallelism. In particular, we demonstrate how to leverage pipeline parallelism via a novel approach of executing backpropagation for the early-exit training loss through pipeline stages. Next, we show (in Section 4.2) how to maximize training efficiency via various performance optimizations, e.g. choosing wisely where to add early exits, and scheduling computation in the correct order. By leveraging idle computational resources in pipeline parallelism, training an early-exit LLM bears negligible overhead compared to training a standard LLM, as confirmed by our analytical and empirical study. Finally, we explore (in Section 4.3) some advanced features implemented in EE-LLM, including the option to change the weights of early-exit losses during the training process, and a novel approach of improving hardware utilization by filling pipeline bubbles with useful computation for additional microbatches.

4.1 Backpropagation through pipeline stages

The standard objective function for training an early-exit model is a weighted sum of losses at early and final exits. More formally, to train an early-exit LLM with N exits (including the final output), we aim to solve

$$\min \mathcal{L} := \sum_{i \in [N]} w_i \mathcal{L}_i^{\text{exit}}, \quad (1)$$

where $[N] = \{1, 2, \dots, N\}$, and each $\mathcal{L}_i^{\text{exit}}$ is a standard loss function for LLM pre-training (e.g. negative log-likelihood of next-token prediction), calculated with outputs from the i -th exit. The loss weights $\{w_i\}$ are hyperparameters specified by the user.

Our implementation of training, i.e. optimizing the loss function in Eq. (1), is compatible with all types of parallelism in Megatron-LM. Indeed, with some engineering efforts, existing functionalities in Megatron-LM for data and tensor/sequence parallelism are directly applicable. The major challenge lies in *pipeline parallelism*, since it is not immediately clear how to calculate gradients for Eq. (1) via backpropagation through pipeline stages. In a single-GPU scenario with vanilla PyTorch, one simply needs to define `loss` as the weighted sum of all early-exit and final-exit losses, and then run `loss.backward()` for gradient calculation. This is obviously not feasible with pipeline parallelism, since losses $\{\mathcal{L}_i^{\text{exit}}\}$ are located on different pipeline stages, and there is only limited P2P communication between each pair of adjacent stages (as explained in Section 2.3). On the other hand, Megatron-LM only supports backpropagation for a single loss function defined in the last pipeline stage.

4.1.1 Methodology

To tackle this challenge, we propose a simple yet effective algorithm that instructs each pipeline stage to calculate the desired gradients correctly, without any additional communication overhead between stages. To explain our method, let us first re-write the early-exit training loss defined in Eq. (1) as

$$\mathcal{L} = \sum_{i \in [K]} \mathcal{L}_i, \quad (2)$$

where K represents the number of pipeline stages, and each \mathcal{L}_i is itself a weighted sum of one or multiple early/final-exit losses within Stage i .² Consider one data sample \mathbf{x} for simplicity, and each loss function is calculated with \mathbf{x} , i.e. $\mathcal{L}_i = \mathcal{L}_i(\mathbf{x})$; in addition, let \mathbf{x}_i be the hidden states that Stage i calculates and sends to its next stage during the forward step. Then, during the backward step, Stage i receives some gradient tensor \mathbf{g}_i from Stage $i + 1$, defines some *auxiliary loss* $\mathcal{L}_i^{\text{aux}}$, and performs usual backward computation for $\mathcal{L}_i^{\text{aux}}$. The auxiliary losses $\{\mathcal{L}_i^{\text{aux}}\}_{i \in [K]}$ and gradient tensors $\{\mathbf{g}_i\}_{i \in [K-1]}$ are defined inductively:

$$\mathcal{L}_K^{\text{aux}} := \mathcal{L}_K, \quad \text{and} \quad (3a)$$

$$\mathcal{L}_i^{\text{aux}} := \mathcal{L}_i + \langle \mathbf{g}_i, \mathbf{x}_i \rangle, \quad \text{where} \quad \mathbf{g}_i := \frac{\partial \mathcal{L}_{i+1}^{\text{aux}}}{\partial \mathbf{x}_i}, \quad i = K - 1, K - 2, \dots, 2, 1. \quad (3b)$$

²It is easy to check that this is equivalent to the loss defined in Eq. (1). In fact, each \mathcal{L}_i can be a general objective function, as long as it is defined locally in Stage i ; our analysis in the following still holds true in this general case.

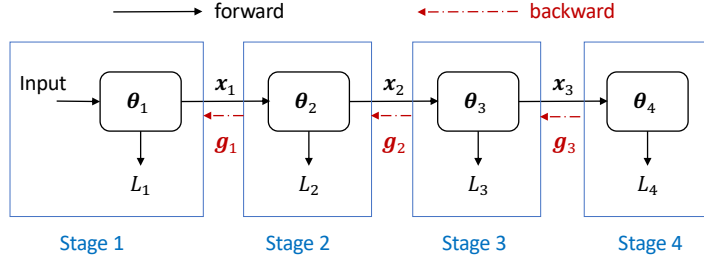


Figure 2: A high-level visualization for the process of backpropagation, including forward and backward passes, for an early-exit model partitioned into four pipeline stages.

Intuitively, the linear term $\langle \mathbf{g}_i, \mathbf{x}_i \rangle$, i.e. the sum of entrywise product between \mathbf{g}_i and \mathbf{x}_i , summarizes information about the gradients of all losses located in later stages. Note that \mathbf{g}_i is regarded by Stage i as a constant tensor, and no gradient is calculated with respect to it.

A visualization of this process can be found in Figure 2. It has the same P2P communication scheme as in the case of training a standard LLM with pipeline parallelism; the only difference is how each gradient tensors \mathbf{g}_i is defined locally in Stage $i + 1$. In the following, we formally prove that the proposed method leads to correct gradient calculation for the training objective in Eq. (2).

4.1.2 Rationale

Let us first prove the correctness of our solution under the assumption that there is no tied/shared parameter across pipeline stages, just for simplicity; we will see very soon that this assumption is not essential and can be safely discarded.

Proposition 1. *Suppose that there is no tied/shared parameter across pipeline stages, and consider the auxiliary losses defined in Eq. (3). Then, for any $i \in [K]$ and any model parameter or activation tensor \mathbf{z} in Stage i , it holds that*

$$\frac{\partial \mathcal{L}_i^{\text{aux}}}{\partial \mathbf{z}} = \frac{\partial (\sum_{j=i}^K \mathcal{L}_j)}{\partial \mathbf{z}}. \quad (4)$$

Notice that for any model parameter \mathbf{z} in Stage i , one has $\partial \mathcal{L}_j / \partial \mathbf{z} = \mathbf{0}$ for any $j < i$, due to the sequential structure of early-exit LLMs (or other deep neural networks). Combining this with Eq. (2) and (4) yields

$$\frac{\partial \mathcal{L}_i^{\text{aux}}}{\partial \mathbf{z}} = \frac{\partial (\sum_{j=i}^K \mathcal{L}_j)}{\partial \mathbf{z}} = \frac{\partial \mathcal{L}}{\partial \mathbf{z}},$$

which implies the correctness of gradient calculation for the training objective \mathcal{L} .

Proof of Proposition 1. The claim of Eq. (4) is obviously true for the base case $i = K$, by definition of $\mathcal{L}_K^{\text{aux}} = \mathcal{L}_K$. Let us prove by induction for the remaining stages. Suppose that Eq. (4) holds true for Stage $i + 1$, namely

$$\frac{\partial \mathcal{L}_{i+1}^{\text{aux}}}{\partial \mathbf{z}} = \frac{\partial (\sum_{j=i+1}^K \mathcal{L}_j)}{\partial \mathbf{z}}.$$

To prove Eq. (4) for Stage i , first note that by definition of \mathbf{g}_i , we have

$$\mathbf{g}_i = \frac{\partial \mathcal{L}_{i+1}^{\text{aux}}}{\partial \mathbf{x}_i} = \frac{\partial (\sum_{j=i+1}^K \mathcal{L}_j)}{\partial \mathbf{x}_i}.$$

Then, for any model parameter or activation tensor \mathbf{z} in Stage i , the following holds:

$$\frac{\partial \mathcal{L}_i^{\text{aux}}}{\partial \mathbf{z}} = \frac{\partial (\mathcal{L}_i + \langle \mathbf{g}_i, \mathbf{x}_i \rangle)}{\partial \mathbf{z}} = \frac{\partial \mathcal{L}_i}{\partial \mathbf{z}} + \frac{\partial \langle \mathbf{g}_i, \mathbf{x}_i \rangle}{\partial \mathbf{x}_i} \frac{\partial \mathbf{x}_i}{\partial \mathbf{z}} = \frac{\partial \mathcal{L}_i}{\partial \mathbf{z}} + \mathbf{g}_i \frac{\partial \mathbf{x}_i}{\partial \mathbf{z}}$$

$$= \frac{\partial \mathcal{L}_i}{\partial \mathbf{z}} + \frac{\partial(\sum_{j=i+1}^K \mathcal{L}_j)}{\partial \mathbf{x}_i} \frac{\partial \mathbf{x}_i}{\partial \mathbf{z}} = \frac{\partial \mathcal{L}_i}{\partial \mathbf{z}} + \frac{\partial(\sum_{j=i+1}^K \mathcal{L}_j)}{\partial \mathbf{z}} = \frac{\partial(\sum_{j=i}^K \mathcal{L}_j)}{\partial \mathbf{z}}.$$

The above lines simply follow the definition of $\mathcal{L}_i^{\text{aux}}$ and the chain rule. This concludes our proof of Eq. (4) for Stage i , and thus our proof for the proposition. \square

Let us move on to relax the assumption. In the broader scenario with tied/shared model parameters (e.g. word embedding matrices [54]) across pipeline stages, gradient calculation via backpropagation is equivalent to the following two-step procedure (as is implemented in Megatron-LM): (1) compute gradients *as if* all parameters are untied, then (2) sum up and synchronize gradients for tied parameters via all-reduce operations. Hence our proposed auxiliary-loss approach, when applied to the first part of the above two-step procedure, is still valid.

4.1.3 Choices of pipeline schedules

Our previous analysis shows how to modify the forward and backward steps for *each* microbatch, in order to execute backpropagation of the early-exit training loss through pipeline stages. In principle, this lightweight modification can be applied to general pipeline schedules of forward and backward steps for *multiple* microbatches. The classical 1F1B (one-forward-one-backward) schedule, also called PipeDream-Flush [47, 20, 49], achieves a good balance of algorithmic simplicity, training time, memory usage and communication latency, in comparison to other schedules such as GPipe [28] (larger activation memory) and interleaved 1F1B [49] (higher memory and communication requirements). Therefore, we focus on the 1F1B schedule throughout this work, for concreteness; a visualization can be found in Figure 3(a).

4.2 Training efficiency

In the following, we analyze the training time and peak GPU memory of training an early-exit model with pipeline parallelism, and propose some performance optimizations. We refer readers to the literature (e.g. the Megatron-LM series [67, 49, 36]) for thorough study of training efficiency with 3D parallelism for standard LLMs without early exits; we will use that as a baseline, and focus on the additional computational overhead caused by early exits.

Let us first identify the major sources of low resource utilization in the original 1F1B pipeline schedule for training a standard LLM, which lays the foundation for our analysis later.

- **Explicit bubbles**, i.e. light gray areas in Figure 3(a), during which GPUs are idle. This is the most notable and well recognized source of low resource utilization in pipeline parallelism.
- **Implicit bubbles**, i.e. dark gray areas in Figure 3(a). This is caused by load imbalance across pipeline stages, even though Transformer layers are evenly divided into stages in Megatron-LM³. In particular, the first stage has the additional computation for the input embedding layer, and more importantly, the last pipeline stage has the additional computation for the output logits (via the output embedding layer) as well as the training loss. For LLMs, these additional computational costs are not negligible, primarily due to large vocabulary sizes.
- **Idle memory**. Memory usage is also imbalanced across pipeline stages: earlier stages in the 1F1B schedule have to save the intermediate activations for more microbatches, and the first/last stage has to save an extra input/output embedding layer, plus the corresponding gradients and optimizer states. As a result, the first stage is typically the bottleneck of peak memory usage, while later stages have idle memory [36, Section 4.2.3].

Remark 1. In our analysis, we assume no activation recomputation [10, 36] for simplicity. For clarity, we also ignore the P2P communication latency between pipeline stages, which is generally not the major concern for efficiency of pipeline parallelism.

³For simplicity, we do not consider other flexible ways of dividing a LLM into pipeline stages, as dividing Transformer layers evenly remains one of the most practical and robust option in practice. We also do not consider the case where the input/output embedding matrix occupies a separate pipeline stage, although our techniques for training an early-exit LLM can be generalized to this case in principle.

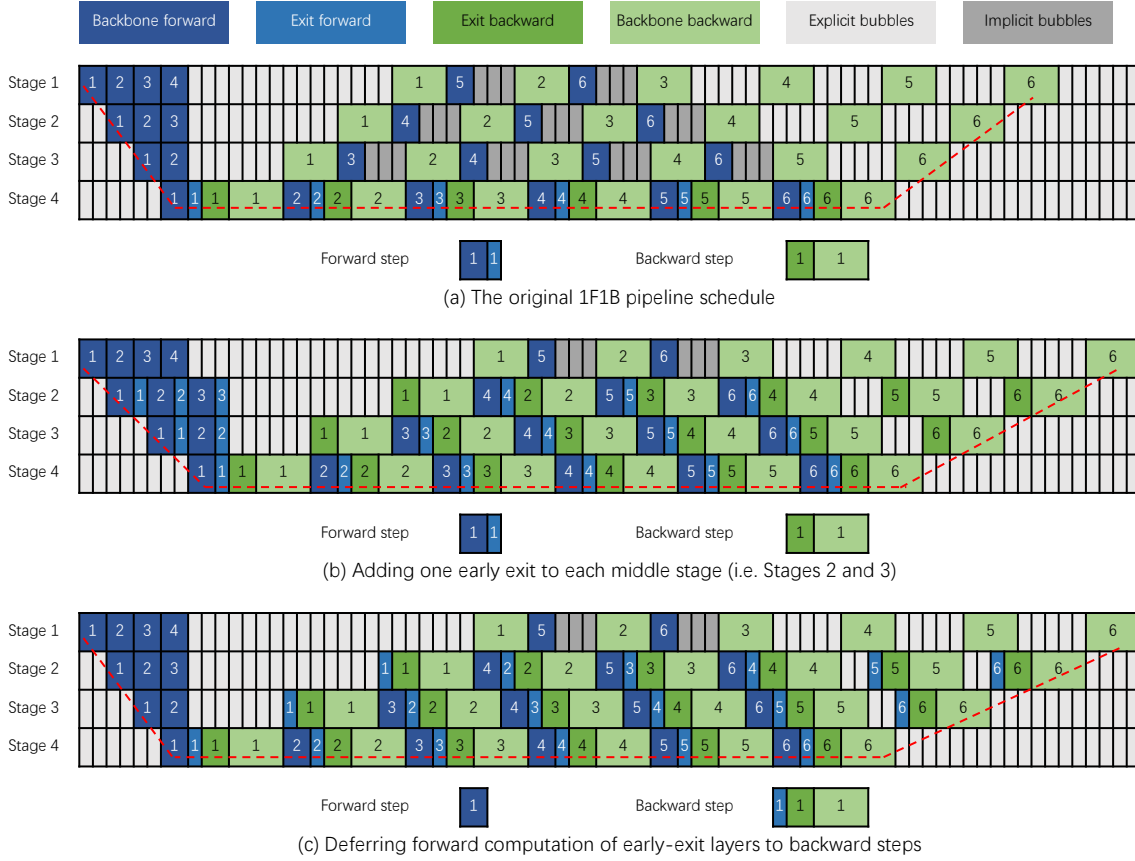


Figure 3: One iteration of the 1F1B pipeline schedule in different cases. Within one iteration, each stage goes through a *warm-up* phase (forward steps of the beginning microbatches), a *steady* 1F1B (one-forward-one-backward) phase, and a *cool-down* phase (backward steps of the final microbatches). “Backbone forward/backward” stands for computation of Transformer layers on the backbone, while “Exit forward/backward” stands for computation of early-exit or final-exit layers. The number in each block denotes the index of the corresponding microbatch. Critical paths are marked by dashed red lines. In this figure, the degree of pipeline parallelism is set to 4, and each data batch is divided into 6 microbatches. It is assumed that for each stage, the ratio of time between forward computation for the backbone and forward computation for the early/final-exit layer is 2:1; moreover, we adopt the common assumption that the ratio of time between forward and backward computation is 1:2. Note that our analytical study does not rely on the specific values of these ratios. For clarity, we ignore computation related to the input embedding layer, as well as P2P communication latency between pipeline stages.

4.2.1 Utilization of idle resources

At first glance, one might expect that adding early exits to an LLM will incur a training overhead, in terms of time and memory, that is (at least) proportional to the number of additional model parameters. Fortunately, this is not the case for training with pipeline parallelism, based on the above analysis of idle resources in the 1F1B pipeline schedule. Indeed, adding one minimalistic early-exit layer (which, as defined in Section 2.2, has the same structure as the final output layer) to some middle (i.e. not the first or last) stage will only make its model size and theoretical forward/backward time match exactly those of the last stage. Therefore, the aforementioned implicit bubbles and some of the idle memory can be automatically utilized for computation related to the early-exit layers, leading to more balanced load across pipeline stages.

More specifically, the overhead to training time caused by additional early exits can be negligible. If we choose k middle stages and add one minimalistic early-exit layer to each of them, then the training time per iteration, i.e. time for processing one data batch, will (in theory) increase only by $k \times (f_{EE} + b_{EE})$, where f_{EE} and b_{EE} represent the time needed for one forward and backward pass of one microbatch for one minimalistic early-exit layer, respectively. To see this, first notice that the computation of early-exit layers in the steady 1F1B phase can be perfectly fit into the implicit bubbles. Therefore, the critical path remains the same as in the case without early exits, which consists of (1) the forward steps on all stages for the first microbatch, (2) the 1F1B steady phase on the last stage, and (3) the backward steps on all stages for the last microbatch. The early-exit layers, located separately on k middle stages, will cause a $k \times f_{EE}$ overhead to the first part of the critical path, and a $k \times b_{EE}$ overhead to the third part, leading to the aforementioned claim on the overhead to training time. See Figures 3(a) and (b) for a visualization.

4.2.2 Further performance optimizations

Reducing activation memory overhead. So far, we have analyzed training time and memory usage by model parameters. Another major component of memory usage, namely the memory for gradients and optimizer states, can be bounded by the memory for model parameters multiplied by a universal constant. One remaining issue that we have not addressed is the *activation memory* overhead due to early-exit computation. Most notably, the early-exit logits for one microbatch have size $s \times b \times V$, where s is the maximum sequence length, b is the microbatch size, and V is the vocabulary size. If the i -th stage has one early exit, then a vanilla implementation of training with early exits using the 1F1B pipeline schedule (as shown in Figure 3(b)) will cause a significant memory overhead of size $s \times b \times V \times (P - i + 1)$, where $P - i + 1$ is the number of in-flight microbatches [36] for Stage i .

Our solution for resolving this issue is simple: deferring the forward computation of each early-exit layer for each microbatch from the forward step to the corresponding backward step. Note that this is feasible, because forward computation of the next stage only requires as input the hidden states returned by the current stage, while the results of early-exit forward computation are optional. By adjusting the order of computation in this way, it is guaranteed that the early-exit logits for each microbatch are generated, used, and discarded immediately, within the same backward step; consequently, the activation memory overhead due to early-exit logits is reduced from $s \times b \times V \times (P - i + 1)$ to $s \times b \times V$. As long as this amount of memory usage is less than the activation memory of *all* Transformer layers within one stage for one microbatch (and no early exit is added to the first stage), the peak memory across all pipeline stages will stay unchanged, since the first stage remains the bottleneck of memory usage.

Remark 2. One can check that, with the above adjustment, our analysis in Section 4.2.1 about the training time overhead caused by early exits remains valid after minor modifications. More specifically, the time overhead of one training iteration is still $k \times (f_{EE} + b_{EE})$; the only difference is that this whole overhead comes from the backward steps of the last microbatch, i.e. the third part of the critical path in Figure 3(c). One can further reduce this overhead to $k \times b_{EE}$ by moving the forward pass of the early-exit layer on each stage for each cool-down microbatch to the explicit bubble in front of the corresponding backward step (i.e. before communication with the next stage). With that said, our implementation does not include this modification, as it brings limited gains at the cost of complicating our codebase.

Some rules of thumb. Below are some tips for maximizing training efficiency.

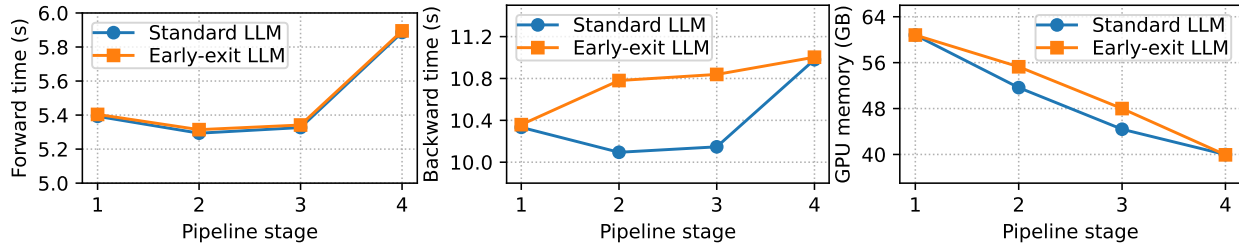


Figure 4: The forward time, backward time, and peak GPU memory of each pipeline stage for a standard 7B GPT Transformer, as well as its early-exit version that has one minimalistic early-exit layer (without layer normalization) added to each middle stage. Degrees of pipeline, tensor and data parallelism are 4, 1, and 1, respectively; the microbatch size is 2, global batch size is 128, and sequence length is 2048. Note that the forward computation of early-exit layers has been deferred to the backward steps, hence not included in “forward time” of the first plot, but in “backward time” of the second plot.

- If possible, add early exits to the middle stages rather than to the first or last one. For example, adding one early exit to the end of the first stage leads to the same model architecture as adding to the beginning of the second stage, but the latter has higher training efficiency due to more balanced load across stages.
- Avoid adding too many early exits to the LLM. Despite higher flexibility during inference, the gain of adding many early exits (e.g. one per layer) might be marginal, and comes at the cost of excessive overhead for training and inference, which is especially the case for LLMs due to large vocabulary sizes. Similar observations and advice have been made recently by the authors of [3] as well.
- If there are multiple exits within the same pipeline stage, one might use the same output embedding matrix for all exits; similarly, if early exits are added to the first/last stage, one might reuse the original input/output embedding matrix for early exits. These choices reduce the memory usage by model parameters, at the cost of lower expressivity of early exits.

Remark 3. Recall from Section 3.1 that, with EE-LLM, users can choose more expressive and powerful early-exit layers beyond the minimalistic structure. Similarly, more than one early exit can be added to each pipeline stage, which provides more flexible choices of exits during inference. These benefits, of course, come at the cost of higher overhead for training, and potentially for inference as well⁴; with EE-LLM, users can conveniently choose the most suitable configurations for their own use cases. We refer interested readers to Appendix A for formal analysis of training efficiency in these general cases.

Numerical examples. We complement previous analytical study with a few numerical examples. Figure 4 illustrates load imbalance in the original 1F1B pipeline schedule for a standard 7B GPT Transformer, as well as the impacts of adding one minimalistic early-exit layer to each middle stage (with all performance optimizations applied). Table 1 takes a close look at the impacts of each performance optimization; unsurprisingly, the best training efficiency is achieved with all the proposed optimizations applied.

4.3 Advanced features

EE-LLM incorporates some advanced features that can potentially improve the training process, which are introduced below. We note that these are exploratory functionalities, and formal investigation of their practical benefits is left for future work.

⁴There is no clear answer to whether additional modules at early-exit layers will improve or hurt the overall inference speed. There is certainly higher overhead for the computation of each early-exit layer; on the other hand, higher flexibility and adaptivity of the early exits can potentially enable them to produce better outputs and get selected more often during inference, leading to overall faster generation of a complete sequence. For similar reasons, there is no clear positive or negative correlation between the number of early exits and the overall speed of generating a sequence.

Table 1: Training efficiency and impacts of performance optimizations, with the same setting as in Figure 4. For the ‘‘Early-exit’’ row, the early exit at 1/4 depth is added to the end of Stage 1, and the exit at 1/2 depth is added to the end of Stage 2. The last three rows are annotated with the performance optimization(s) adopted, where Optimization 1 stands for deferring forward computation of early-exit layers to backward steps, and Optimization 2 stands for moving every early exit from the end of some pipeline stage to the beginning of the next stage, in order to achieve more balanced load across stages. Stage 1 is the bottleneck of peak memory in most cases, except for the numbers marked by *, for which Stage 2 is the bottleneck.

Setup	1.3B		7B	
	Time per iteration (s)	Peak memory (GB)	Time per iteration (s)	Peak memory (GB)
Standard	5.23	19.85	17.75	62.27
Early-exit	5.31	24.05	17.93	67.42
Early-exit (1)	5.29	22.56	17.91	65.79
Early-exit (2)	5.28	20.23 *	17.81	62.27
Early-exit (1&2)	5.24	19.85	17.79	62.27

4.3.1 Non-constant weights of early-exit losses

The weights of early-exit losses in the training objective of Eq. (1) can be changing rather than constant during the training process, just like the learning rate or other hyperparameters. Allowing the weights to be changing can offer a more fine-grained control of how gradients from multiple loss functions jointly impact the backbone and early/final output layers of the model. This functionality has been implemented in EE-LLM.

One concrete option that we offer is *warm-up*. With this option, early-exit loss weights start at small values, and gradually increase with training iterations until reaching the pre-specified maximum values. This approach has been adopted in prior works [31]. The idea is to encourage the deep neural network to primarily optimize for the full-model output quality from the beginning of the training process, while the skill of early exiting is gradually acquired with minor or no negative impact on the final outputs of the full model.

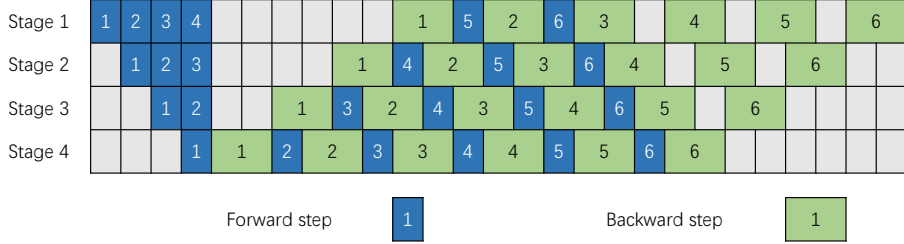
Another option is *cool-down*, which does the opposite and decreases early-exit loss weights during the training process. This option is inspired by prior works [39, 69] that leverage early-exit losses for the purpose of regularizing the training process of deep neural networks. Such ‘‘deep supervision’’ provided by early-exit losses can stabilize and accelerate convergence of training, and potentially improve the intermediate features learned by the neural network. As early-exit loss weights gradually decay, the regularization gets weaker, so that the network becomes more focused on its primary objective, namely the final-output quality.

4.3.2 Filling explicit bubbles with additional microbatches

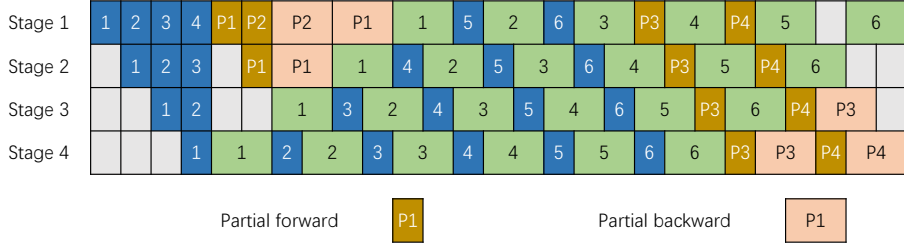
To further leverage the explicit bubbles within the 1F1B pipeline schedule, i.e. the gray areas in Figure 5, we design and implement a novel approach of filling them with *partial* forward/backward computation of additional microbatches. This is primarily inspired by the idea from [51]: instead of designing a new, sophisticated pipeline schedule that has a lower bubble ratio, one may seek to fill the bubbles of an existing schedule with useful computation, which can lead to better resource utilization and faster training.

Our approach is visualized in Figure 5 and explained below. For notational simplicity, let us call the explicit bubbles between the warm-up and steady phases as Part 1, and the bubbles during the cool-down phase as Part 2. For each part, we fill them with some computation for K additional microbatches. More concretely, for Part 1, the i -th inserted microbatch (where $i \in [K]$) goes through forward computation of the first $K + 1 - i$ pipeline stages, followed by backward computation of all visited early-exit losses; for Part 2, each inserted microbatch goes through forward computation of all stages, followed by backward computation of the final and early-exit losses (if any) only for the last few stages. In this way, each training iteration can process more data without any time overhead, as long as the number of inserted microbatches and the number of stages for partial forward/backward computation are chosen appropriately.

One thing to note is that this approach changes the optimization semantics. From the perspective of stochastic optimization, we can prove formally that with such additional computation and under certain conditions, one obtains an *unbiased* gradient estimate with *reduced variance* for the original training objective. We refer interested readers to Appendix B for more details about the methodology and analysis.



(a) The original 1F1B pipeline schedule



(b) Filling explicit bubbles with additional microbatches

Figure 5: A visualization for our proposed method of filling pipeline bubbles with partial forward and backward computation of four additional microbatches, i.e. the ones annotated as P1, P2, P3 and P4.

5 Inference

This section first explains the major challenge faced by early-exit inference of LLMs in autoregressive generation tasks, namely the conflict between early exiting and KV caching, as well as a few recent attempts to resolve it. Then, we introduce our novel approach, which is based on a new type of pipeline parallelism. Throughout this section, we focus on the latency-oriented setting, with a batch size of 1 during sequence generation.

5.1 Main challenge: KV caching

Accelerating inference with early exiting is, in principle, orthogonal to and compatible with many other common techniques of acceleration [32], such as kernel fusion, FlashAttention [15], model quantization [85, 80], among others. For autoregressive generation tasks, one exception is KV caching, i.e. saving keys and values of all attention layers for previously generated tokens, which accelerates sequence generation by reducing redundant computation (though at the cost of higher memory usage). This is obviously in contradiction with vanilla early-exit inference: if the current token is generated via early exiting, then its KV caches in later layers are missing, which hinders the generation of future tokens that go beyond the exiting layer of the current token.

This challenge has been well recognized in the literature, and several approaches have been recently proposed to resolve it. One approach [19, 42, 61] is to copy the hidden states of the current token at the exiting layer to all later layers, which will be used to compute the keys and values at later attention layers. Despite its efficiency, this method obviously causes a deviation from the inference process that the model is trained to excel at, which can harm the output quality. Another solution [13] is to pre-specify the exiting layer for each token, while ensuring that KV missing in previous tokens will not hinder generation of later tokens; with this approach, the ability of token-wise adaptive selection of exits is inevitably lost. The third method [3, 70] is to store the hidden states of recent tokens that were generated with early exiting, and whenever KV missing happens, run a batch forward pass with the current and recent tokens to fulfill the KV caches. A variant of this approach, which we call KV recomputation, is implemented in EE-LLM; we defer its details to Section 6.3. Despite the batching effect of GPU computation, this approach still brings additional computational overhead, and might not even achieve any acceleration for inference on other hardware platforms, due to its high computational complexity.

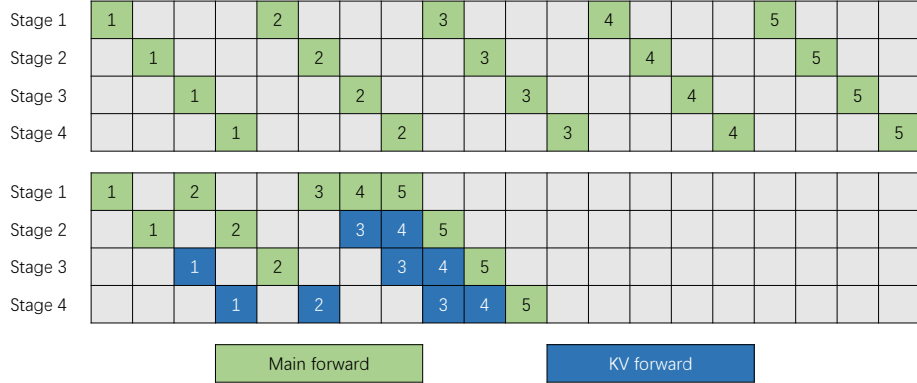


Figure 6: A comparison between the standard full-model inference (top), and our pipeline-based approach of early-exit inference (bottom). Numbers in the blocks represent the tokens within one generated sequence. Here, we consider the special case where each early exit is located at the end of a certain pipeline stage, just for simplicity of visualization.

5.2 A new solution: pipeline parallelism

We propose a novel solution that leverages a new type of pipeline parallelism during inference. The key idea is that, in the process of inference with multiple pipeline stages, the following two processes run *in parallel* whenever the model decides to do early exiting for the current token at a certain early exit:

- The generated token is sent back to the first stage, and the forward pass for generating the next token is started immediately;
- The full-model forward pass of the current token is continued from the exiting layer, which fulfills the KV caches in all later layers.

See Figure 6 for a visualization of our proposed approach. Even though each token essentially goes through a forward pass of the full model, the computation after the exiting layer is *parallelized* with the computation of later tokens, which is how acceleration is achieved in this approach. It can be checked that the inference latency for generating one token at a certain exit matches exactly the time needed for the forward computation before returning an output at that exit, unless the selected exit is located in the middle of the first pipeline stage, in which case generation of the next token has to wait until the forward pass of the first stage for the current token is completed. Note that this is true not just in practice but also for the *theoretical* time complexity, without relying on the batching effect of GPU computation like KV recomputation does.

An implementation of this pipeline-based inference method is provided in EE-LLM. One potential limitation of the proposed method is that it requires multiple devices to facilitate pipeline parallelism, although parallelism within a single GPU or other device might be possible with more advanced implementation.

6 Implementations

The implementation of EE-LLM is based on Megatron-LM [49], primarily extending Megatron-LM’s model architectures, pipeline scheduling, and inference service to support the training and inference of early-exit LLMs. We introduce each of these aspects in more details below.

6.1 Model architectures

We have introduced a new class of models called `EarlyExitGPTModel`, which is the early-exit counterpart of `GPTModel` in the original model library of Megatron-LM. The model is constructed with a few other classes, including `EarlyExitTransformerLayer`, `EarlyExitTransformer`, and `EarlyExitLanguageModel`.

`EarlyExitTransformerLayer` is a replacement for the original `ParallelTransformerLayer` in Megatron-LM. It adds an early-exit structure on top of the standard Transformer layer, which allows it to generate outputs for both the main network backbone and the early exit; for the latter, it returns a lazy loss function during training, or tokens during inference. This module supports various customizations of the early-exit structure; besides the minimalistic structure with an output embedding matrix and an optional output normalization layer, one might add e.g. a MLP or a complete Transformer layer. These additional structures can be combined in any desired manner and can be placed before or after the backbone part of this layer. On the other hand, `EarlyExitTransformer` and `EarlyExitLanguageModel` are mainly used to propagate the early-exit outputs to the top-level model. They are capable of stopping the forward computation at the early-exit layer and returning the intermediate outputs, which facilitates accelerated inference.

6.2 Pipeline scheduling

We have adjusted the existing 1F1B schedule for early-exit LLMs, as shown in Figure 3. To fill implicit bubbles and reduce GPU memory overhead, lazy loss functions of early-exit layers are returned together with outputs of the backbone network during forward steps. These lazy functions are not actually called until their corresponding auxiliary losses (cf. Section 4.1.1) are calculated in the backward steps. For the method of filling explicit bubbles proposed in Section 4.3.2, we have inserted partial forward/backward computation of additional microbatches into warm-up and cool-down phases of the 1F1B schedule. The number of inserted microbatches and partial forward/backward stages can be automatically calculated through the user-specified (estimate of) ratio between backward and forward time.

6.3 Inference service

To support inference of early-exit LLMs, we have refactored the text-generation module of Megatron-LM.

For inference with pipeline parallelism, i.e. the *pipeline-based* approach proposed in Section 5.2, we have re-implemented the forward process. With our implementation, the first pipeline stage will wait for an exit signal from the early/final exits of all subsequent stages after its forward computation is completed. Each subsequent stage will send an exit signal and the output token to the first stage, if there is an exit within the stage that satisfies the exit condition. Upon receiving the signal and generated token, the first stage will immediately start the forward pass for generating the next token. With this implementation, regardless of the early-exit layers’ positions in subsequent stages, the inference service can immediately generate a token whenever early exiting happens on some stage, without waiting for the completion of the entire stage (except for the first stage).

For inference without pipeline parallelism, we have implemented a mechanism of *KV recomputation*, which is a variant of synchronized parallel decoding proposed recently in [3]. In this approach, we maintain a list of the most recent tokens that have missing KV caches in deep layers due to early exiting. During each forward pass, we include these early-exit tokens in the current forward pass, which allows for direct recomputation of the KV caches for these tokens and thus avoids the issue of missing KV caches. Acceleration of sequence generation is still achieved, thanks to the batching effects of GPU computation. To avoid the endless accumulation of early-exit tokens, we enforce a full-model forward pass whenever the number of early-exit tokens reaches a pre-specified value.

7 Experiments

This section provides an empirical evaluation of the training and inference efficiency achieved by EE-LLM.

7.1 Training

In the following experiments, we empirically investigate the convergence of training early-exit models with EE-LLM, as well as the training efficiency of EE-LLM for early-exit LLMs up to an unprecedented scale of 30B. This scale is only limited by the hardware resources available to us, namely an 8-node cluster with 8

Nvidia A100-80GB GPUs in each node and hence 64 GPUs in total. We use a subset of the pre-training data⁵ provided by Data-Juicer [9], which consists of 800 billion tokens.

7.1.1 Convergence of training losses

First of all, we conduct experiments to verify the convergence of training losses when training early-exit LLMs with EE-LLM. We first consider a 1.3B GPT Transformer with 24 layers, add one minimalistic early-exit layer without layer normalization to the 1/4 depth and the other to the 1/2 depth, set their early-exit loss weights to 1/4 and 1/2 respectively (while the final-exit loss has a weight of 1), and tie all input and output embedding matrices. A standard LLM of the same GPT architecture is also trained using the same hyperparameters and pre-training data. We further train a 7B early-exit model with 32 layers using similar configurations, except that early-exit loss weights are set to 0.1 and 0.2, and all embedding matrices are untied. A 7B standard model is trained similarly. In all cases, we use the Adam optimizer [35] with hyperparameters $\beta_1 = 0.9$, $\beta_2 = 0.95$, $\epsilon = 10^{-8}$, and a cosine schedule for the learning rate, with a maximum value of 3×10^{-4} . The batch size and sequence length are both set to 2048.

Figure 7 shows the convergence of early-exit and final-exit training losses, i.e. negative log-likelihood of next-token prediction, for both standard and early-exit LLMs. All loss curves decay at a similar pace, and unsurprisingly, the early-exit losses are slightly higher than the final-exit loss for each model. Interestingly, the final-exit loss curve of each early-exit model is close to (or even slightly below) that of the standard model, suggesting that optimizing for early-exit losses might not hurt the final output of the full model in our setting. We also observe more spikes in the loss curves for the 7B model than for the 1.3B models, possibly due to the following reasons: (1) we choose to untie the embedding matrices and use smaller early-exit loss weights, both of which incur weaker regularization for the training process; (2) layer normalization, which is known to stabilize training of LLMs, is not included in the minimalistic early-exit layers of our 7B model.

7.1.2 Training efficiency

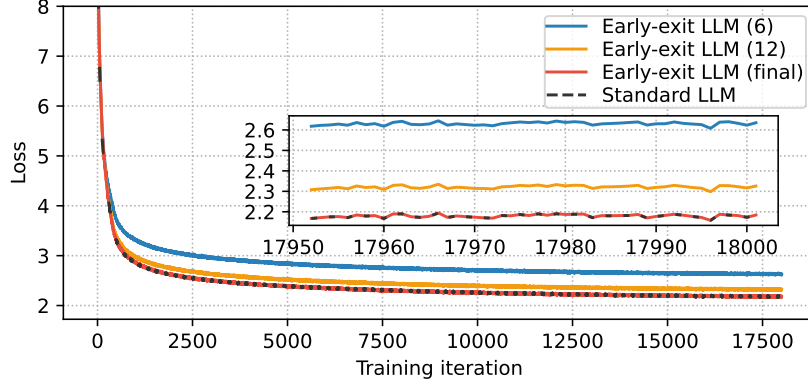
In this experiment, we investigate the training overhead of early exits. Starting with a standard GPT Transformer of size ranging from 1.3B to 30B, we increase the number of early exits from 0 to 3. Minimalistic early exits are added one by one to specific locations in the following order: (1) to the 1/4 depth; (2) to the 1/2 depth; (3) to the hidden states right before the first Transformer layer, which is always located in the first pipeline stage. Based on the performance optimizations proposed in Section 4.2, when an early exit is inserted into the middle of two layers located on two consecutive pipeline stages, we always add it to the beginning of the latter stage. We set the global batch size to 2048, microbatch size to 2 (for 1.3B and 7B models) or 1 (for 13B and 30B models), and sequence length to 2048. The degree of data parallelism is set to 4 and fixed throughout, while tensor/sequence and pipeline parallelism degrees can take various values.

Numerical results are illustrated in Figure 8, which matches the results from our analytical study in Section 4.2. In particular, training time per iteration (i.e. time for processing one data batch) increases with the number of added early exits, but at a slower rate when pipeline parallelism is enabled, thanks to the proposed utilization of implicit bubbles. Without pipeline parallelism, peak GPU memory increases with the number of early exits; on the other hand, with the pipeline parallelism degree set to 4, peak memory remains unchanged as early exits are added to middle pipeline stages, and only increases when the last early exit is added to the first stage, as predicted by our analysis in Section 4.2.

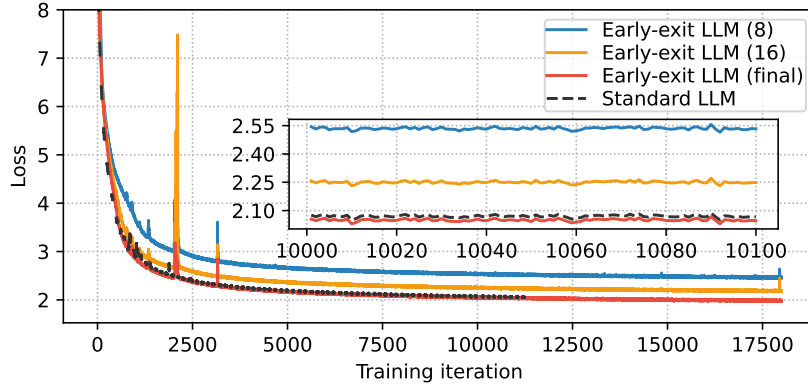
7.2 Inference

In the experiments below, we verify the effectiveness of our pipeline-based approach (with the number of pipeline stages set to 4) proposed in Section 5.2, and the method of KV recomputation explained in Section 6.3, for autoregressive generation with early exiting. Given that both methods generate the same output for the same prompt, we first investigate the downstream performance and early-exit speedup for the pipeline-based method alone, and then compare the inference speed of both methods. A server with 4 Nvidia A100-40GB GPUs is used for inference.

⁵https://github.com/alibaba/data-juicer/blob/main/configs/data_juicer_recipes/README.md



(a) 1.3B, 24 layers



(b) 7B, 32 layers

Figure 7: Convergence of early-exit/final-exit training losses for our Transformer models. Each curve is annotated with the index of the Transformer layer that the corresponding exit is connected to.

To examine the performance of inference with various sizes of models, we conduct experiments under different settings. One model that we use is an 1.3B early-exit model pre-trained from scratch with 300B tokens, and the other one is a 7B model pre-trained with 150B tokens. Each of them has two minimalistic early exits added to the 1/4 and 1/2 depth respectively; other configurations follow those in Section 7.1.1. Neither model has gone through any fine-tuning or alignment. Since designing the decoding method or early-exit condition is not the focus of our work, we simply adopt greedy decoding and a basic confidence-based decision rule for early exiting: at each early exit, if the maximum probability of next-token prediction is above a pre-defined threshold, then the model chooses the most likely token and moves on to generate the next one. The trade-off between output quality and speed of generation is then controlled by the threshold. Note that for a fair comparison, when the threshold is set to 1, early-exit layers are disabled, so that the computational complexity of a full-model forward pass matches that of a standard LLM without early exits; the inference latency with the threshold set to 1 is also used as the baseline for calculating (relative) speedup.

7.2.1 Output quality and speed of generation

We evaluate the downstream performance of our models with HELM [43] in four tasks. Among them, BoolQ [12] and TruthfulQA [44] are question-answering tasks, while XSUM [46] and CNN/DailyMail [64] are summarization tasks. We use EM (ratio of exact match with the correct answers) as the metric for the former, and ROUGE-L (a measure of similarity to the reference summaries) for the latter. Figure 9 demonstrates the relation between scores and inference speedup for pipeline-based inference with varying thresholds. Encouragingly, for many of these tasks, inference with early exiting can achieve 2× or higher speedup compared to full-model inference, with comparable or even better evaluation scores. Table 2 provides a concrete piece of text generated by our 7B early-exit model, showing that speedup can be achieved with

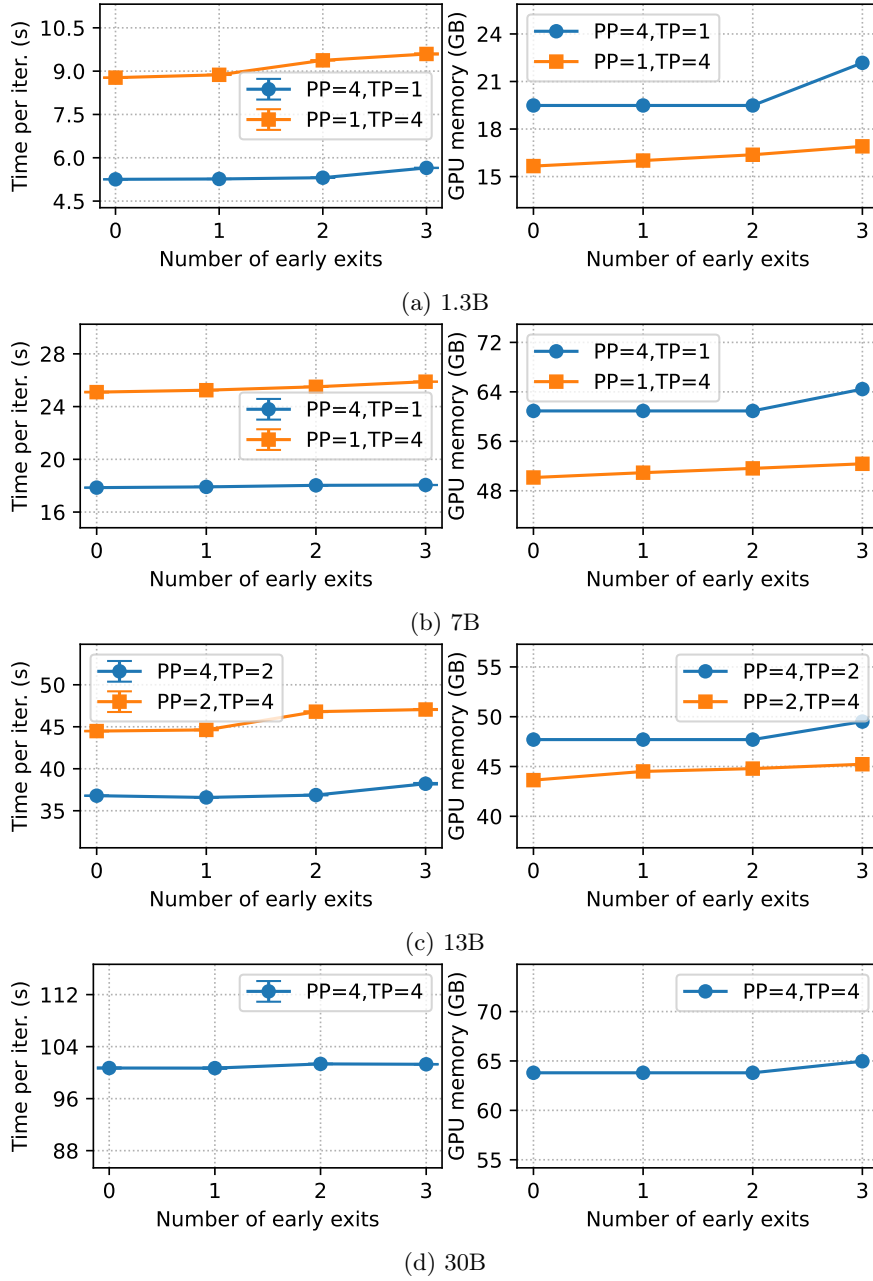


Figure 8: Training time per iteration and peak GPU memory vs. the number of added early exits, under various configurations of model sizes and parallelism degrees. Note that wall-clock time can be impacted by other workloads on the same GPU cluster when our experiments were conducted, which inevitably causes perturbations to our numerical results.

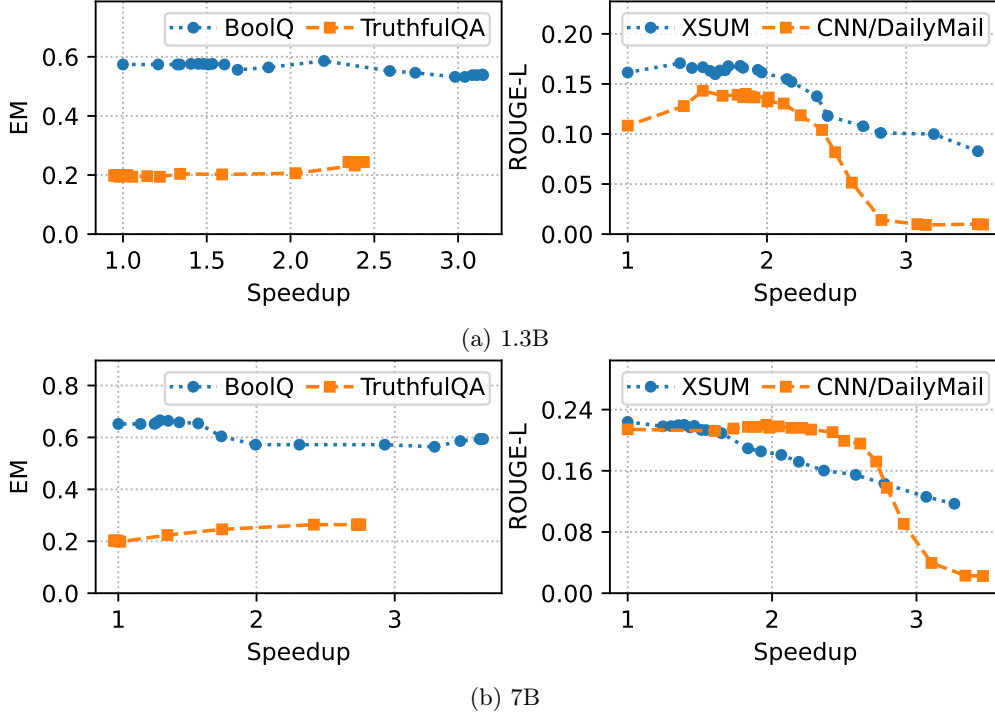


Figure 9: Evaluation scores and relative speedup with our early-exit models. For each curve, the confidence threshold decreases from left to right.

minor or no impact on the resulted sequence. Table 3 goes one step further and demonstrates the confidence at each exit for each token, confirming the existence of easy tokens that can be predicted with high confidence at early exits, without wasting computational resources on later layers. It is worth noting that performance of early-exit inference might be improved in many ways, e.g. using early exits of different structures, other decoding mechanisms and exit conditions, or simply more extensive and sufficient pre-training. We also conjecture that early exiting can, in principle, bring higher speedup for larger models, as expressivity of early exits grows with the model capacity, which allows them to make confident and accurate predictions for a larger proportion of tokens.

7.2.2 A comparison between two inference methods

We compare the inference time of both pipeline-based method and KV recomputation. Since the pipeline-based method uses 4 GPUs for a pipeline parallelism (PP) degree of 4, we allow KV recomputation to use a tensor parallelism (TP) degree of 1 or 4 for a fair comparison. The empirical results on XSUM and CNN/DailyMail tasks are shown in Figure 10. We first notice that the pipeline-based approach outperforms KV recomputation with TP = 1 for confidence thresholds smaller than 1 (i.e. when early exiting actually happens), despite the point-to-point communication overhead. Moreover, KV recomputation with TP = 4 is faster than the pipeline-based approach; it is worth noting, however, that the small speedup from TP = 1 to TP = 4 for KV recomputation is only possible with high-end hardware like A100 GPUs connected by high-bandwidth communication. In many use cases of LLM inference, such hardware is not available, and pipeline parallelism is the only option for partitioning a model that is too large to fit into the memory of one single device. In sum, the proposed pipeline-based approach is a more practical option for LLM inference with model partitioning in a wide range of scenarios.

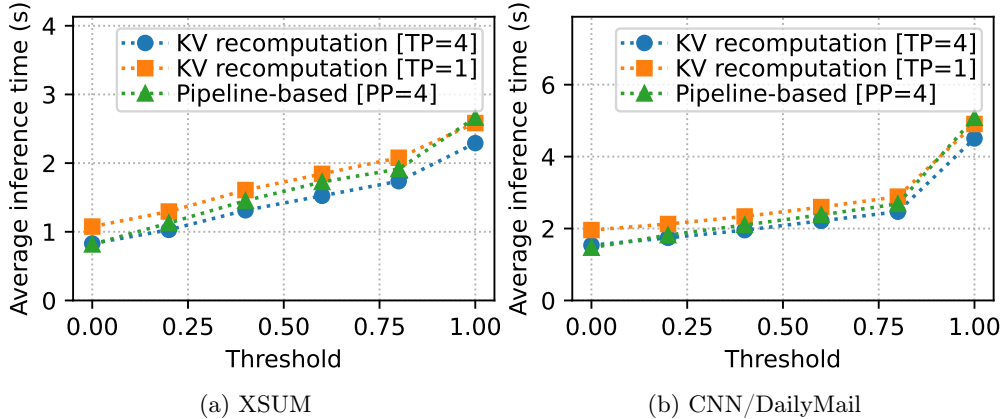


Figure 10: A comparison of inference speed between the pipeline-based method (with 4 pipeline stages) and KV recomputation (with the degree of tensor parallelism set to 1 or 4) for our 7B early-exit model.

8 Related works

As introduced in Section 1, early exiting has been widely applied for accelerating inference of deep neural networks in the literature. In terms of early-exit Transformers in the NLP domain, the majority of prior works is focused on BERT [16] or other encoder-only models for classification tasks [45, 25, 94, 19, 63, 81, 62, 82, 42, 26]. Recent works have begun to study token-wise early exiting for accelerating inference of encoder-decoder or decoder-only LLMs in autoregressive sequence generation [62, 13, 3, 76]. While they are largely focused on designing *inference* mechanisms, the lack of support in prior works for *training* early-exit models with massive 3D parallelism inevitably posts an obstacle towards truly scaling up early-exit LLMs. Our work on EE-LLM is one important step towards eliminating this obstacle, and we also contribute a novel pipeline-based inference mechanism along the way.

Interestingly, early exiting has been used for many other purposes in the literature, besides accelerating inference. For example, early-exit losses can provide deep supervision and regularization for training deep networks with enhanced stability of convergence [69, 39], which motivates our implementation of the cool-down option for non-constant early-exit loss weights, as explained in Section 4.3.1. Other works use early exits for interpreting the intermediate features learned by each layer of a Transformer [37], for improving outputs of the final exit [22], or as the draft models in speculative decoding [33]. Early exiting has also found application in long-tailed classification [18], federated learning with heterogeneous clients [29, 93], token reduction [1], layer-wise training of deep networks [60, Section 5.3], among others. We believe that our progress in this work can be beneficial for these various purposes.

It is worth mentioning that there are other types of dynamic neural networks [24, 83] that facilitate conditional computation and elastic inference, such as layer skipping [6, 5, 79, 13, 17, 87, 78] and mixtures of experts [30, 66, 21]. Another line of work aims to accelerate LLM inference by designing new decoding methods rather than model architectures [40, 59, 91]. Each of these approaches has its own pros and cons, and some of them can be complemented by early exiting. A detailed comparison between these methods is beyond the scope of the current work.

9 Conclusions

We have introduced EE-LLM, a system for large-scale training and inference of early-exit LLMs with 3D parallelism. For training, we have presented how to execute backpropagation of the early-exit training objective across pipeline stages, various performance optimizations for minimizing the computational overhead compared to training standard LLMs, and some advanced features for more fine-grained control and optimization of the training process. For inference, we have introduced our design and implementation of two inference methods, one based on KV recomputation and the other based on a new type of pipeline parallelism, both of which are compatible with KV caching for autoregressive generation. Along the way, we have discovered

Table 4: A list of notation for theoretical analysis. The following abbreviations are used: IN — input processing layer; EE — early-exit layer; FE — final-exit layer; BB — Transformer backbone on one pipeline stage.

Notation	Definition
P	Number of pipeline stages
N_i	Number of early exits in Stage $i \in [P]$
M	Number of microbatches for one training iteration
f_o, b_o	Forward and backward time of one $o \in \{\text{IN}, \text{EE}, \text{FE}, \text{BB}\}$ for one microbatch
m_o	Memory usage for storing the model parameters of one $o \in \{\text{IN}, \text{EE}, \text{FE}, \text{BB}\}$
m_o^\dagger	Activation memory of one $o \in \{\text{IN}, \text{EE}, \text{FE}, \text{BB}\}$ for one microbatch
$\mathbb{1}(\cdot)$	The indicator function, $\mathbb{1}(\mathcal{E}) = 1$ if the event \mathcal{E} holds true, and 0 otherwise

some interesting chemical reaction between early exiting and pipeline parallelism, which is likely because it is both along the depth dimension that an early-exit model executes forward computation selectively and gets partitioned by pipeline parallelism. With EE-LLM, it now becomes possible to train and deploy early-exit LLMs that are as large as any standard LLM allowed by Megatron-LM, given the same amount of computational resources. We hope that EE-LLM will be a helpful tool for future study and applications of early-exit LLMs at larger scales.

At the time of writing this article, we are continuously updating our codebase with more thorough experiments and more advanced functionalities. It is worth noting that many ideas presented in this work can be generalized to broader settings, e.g. deep neural networks other than decoder-only GPT Transformers, frameworks other than Megatron-LM, and hardware platforms other than GPU clusters; it would be exciting to see further developments in these aspects.

A Analysis of training efficiency

In this section, we derive formulas for the training time per iteration and peak GPU memory usage across pipeline stages under general configurations of early exits, in terms of the quantities listed in Table 4. Some of these quantities, especially $\{f_o, b_o, m_o, m_o^\dagger\}$, can be further calculated analytically with lower-level quantities such as sequence length, microbatch size, hidden size, vocabulary size and others [57, 49, 36], or estimated empirically by profiling in practice.

It is assumed that all pipeline stages have the same number of Transformer layers on the backbone, and all early-exit layers follow the same structure. We also assume that input and output embedding matrices are untied, although it is not hard to extend our analysis to more general cases. For simplicity, we ignore the point-to-point communication latency between pipeline stages in our analysis, since it typically takes a minor proportion of the overall training time, and can often be overlapped with computation.

A.1 Training time per iteration

Let us analyze the training time per iteration step by step.

Step 1: simplified analysis without early exits. We start by recalling the simplified analysis in prior works for the standard 1F1B pipeline schedule [49], which assumes that all stages have the same forward time f and backward time b for one microbatch. Recall from Figure 3 that the critical path of one training iteration consists of three parts:

- Part 1: forward steps of the first microbatch on all stages except the last one, which takes time $(P - 1) \times f$;
- Part 2: the steady 1F1B phase with all M microbatches on the last stage, which takes time $M \times (f + b)$;
- Part 3: backward steps of the last microbatch on all stages except the last one, which takes time $(P - 1) \times b$.

Taking the sum of these three parts, we have

$$\text{time per iteration} = (P-1) \times f + M \times (f+b) + (P-1) \times b = \underbrace{(P-1) \times (f+b)}_{\text{Parts 1 and 3}} + \underbrace{M \times (f+b)}_{\text{Part 2}}.$$

Step 2: fine-grained analysis without early exits. We provide a more fine-grained analysis, by considering the computation related to the input processing layer (IN) and final-exit layer (FE) separately from the Transformer backbone (BB). It is reasonable to assume that $f_{\text{IN}} < f_{\text{FE}}$ and $b_{\text{IN}} < b_{\text{FE}}$, which implies that the last stage is the bottleneck of forward and backward time. In this setting, Parts 1 and 3 of the critical path takes time $f_{\text{IN}} + (P-1) \times f_{\text{BB}}$ and $b_{\text{IN}} + (P-1) \times b_{\text{BB}}$, respectively. Similarly, Part 2 now takes time $M \times (f_{\text{BB}} + b_{\text{BB}} + f_{\text{FE}} + b_{\text{FE}})$. Taking the sum, we arrive at

$$\text{time per iteration} = \underbrace{f_{\text{IN}} + b_{\text{IN}} + (P-1) \times (f_{\text{BB}} + b_{\text{BB}})}_{\text{Parts 1 and 3}} + \underbrace{M \times (f_{\text{BB}} + b_{\text{BB}} + f_{\text{FE}} + b_{\text{FE}})}_{\text{Part 2}}.$$

Step 3: fine-grained analysis with early exits. Finally, we are ready for our analysis in the setting with early exits (EE). First, it can be checked that early-exit layers incur a total overhead of

$$\sum_{i \in [P-1]} N_i \times (f_{\text{EE}} + b_{\text{EE}})$$

to Parts 1 and 3. In addition, the sum of forward and backward time of one microbatch for Stage i becomes

$$f_{\text{BB}} + b_{\text{BB}} + \mathbb{1}(i=1) \times (f_{\text{IN}} + b_{\text{IN}}) + \mathbb{1}(i=P) \times (f_{\text{FE}} + b_{\text{FE}}) + N_i \times (f_{\text{EE}} + b_{\text{EE}}).$$

Note that Part 2, namely the steady 1F1B phase on the last stage, is now *bottlenecked* by the maximum forward and backward time across all stages. Putting things together, we have the following upper bound:

$$\begin{aligned} & \text{time per iteration} \\ & \leq f_{\text{IN}} + b_{\text{IN}} + (P-1) \times (f_{\text{BB}} + b_{\text{BB}}) + \sum_{i \in [P-1]} N_i \times (f_{\text{EE}} + b_{\text{EE}}) \\ & \quad + M \times \max_{i \in [P]} \left\{ f_{\text{BB}} + b_{\text{BB}} + \mathbb{1}(i=1) \times (f_{\text{IN}} + b_{\text{IN}}) + \mathbb{1}(i=P) \times (f_{\text{FE}} + b_{\text{FE}}) + N_i \times (f_{\text{EE}} + b_{\text{EE}}) \right\}. \end{aligned}$$

The overhead caused by early-exit layers has been highlighted. The first term corresponds to Parts 1 and 3 of the critical path, and the second term corresponds to Part 2. It is worth mentioning that the second term of the overhead might not take effect due to the maximum operator, in which case the early-exit overhead to one training iteration is independent of the number of microbatches.

A.2 Peak GPU memory

Consider the GPU memory for one specific pipeline stage, say Stage i . Recall that GPU memory usage during training is mainly composed of memory for model parameters, gradients, optimizer states, and intermediate activations [57, 36]. Among them, the memory for gradients and optimizer states (for many common optimizers, such as SGD with momentum or Adam) is proportional to the number of model parameters. Therefore, we assume that

$$\text{memory}(\text{model parameters, gradients, optimizer states}) = \alpha \times \text{memory}(\text{model parameters})$$

for some universal constant $\alpha > 1$, whose concrete value depends on the choice of optimizer and numerical precisions. Under this assumption, we have

$$\text{total memory} \approx \alpha \times \text{memory}(\text{model parameters}) + \text{memory}(\text{activations}). \quad (5)$$

Now it boils down to deriving the memory for model parameters and activations. Model parameters in Stage $i \in [P]$ include the Transformer backbone (BB), the input processing layer (IN) if $i = 1$, the final-exit layer (FE) if $i = P$, and the early exits (EE). In other words, we have

$$\text{memory}(\text{model parameters}) = m_{\text{BB}} + \mathbb{1}(i=1) \times m_{\text{IN}} + \mathbb{1}(i=P) \times m_{\text{FE}} + N_i \times m_{\text{EE}}. \quad (6)$$

The memory for intermediate activations can be similarly divided into components corresponding to BB, IN, FE and EE. Note that according to Section 4.2.2, the peak memory usage by activations within one early-exit layer is only m_{EE}^\dagger regardless of the number of in-flight microbatches $P + 1 - i$. Thus one has

$$\text{memory(activations)} = (P + 1 - i) \times m_{BB}^\dagger + \mathbb{1}(i = 1) \times P \times m_{IN}^\dagger + \mathbb{1}(i = P) \times m_{FE}^\dagger + N_i \times m_{EE}^\dagger. \quad (7)$$

Combining Eq. (6) and (7) with Eq. (5), we arrive at an estimate of memory usage for Stage i :

$$\begin{aligned} \text{total memory} \approx & \alpha \times \left(m_{BB} + \mathbb{1}(i = 1) \times m_{IN} + \mathbb{1}(i = P) \times m_{FE} + N_i \times m_{EE} \right) \\ & + \left((P + 1 - i) \times m_{BB}^\dagger + \mathbb{1}(i = 1) \times P \times m_{IN}^\dagger + \mathbb{1}(i = P) \times m_{FE}^\dagger + N_i \times m_{EE}^\dagger \right). \end{aligned}$$

The memory overhead caused by early-exit layers has been highlighted in red. Finally, taking the maximum over $i \in [P]$ gives the peak GPU memory across all pipeline stages.

B Supplementary materials for Section 4.3.2

This section provides more details about the method, proposed in Section 4.3.2, of filling pipeline bubbles with partial forward/backward computation of additional microbatches.

B.1 Methodology

How many microbatches can be inserted? The maximum number of microbatches that can be inserted into Part 1 or 2 of the explicit bubbles, without increasing training time per iteration, is $\lfloor (p-1)b/(f+b) \rfloor = \lfloor (p-1)/(f/b+1) \rfloor$, where f/b is (an estimate of) the ratio between forward and backward time. To see this for Part 1 (resp. 2), one simply need to notice that the first (resp. last) pipeline stage has an bubble size $b(p-1)$, while the total forward and backward time for each microbatch is $f+b$. Dividing the first value by the second one concludes the proof.

Details about Part 1. With K inserted microbatches, the i -th microbatch is supposed to go through the forward pass of the first $K + 1 - i$ stages. However, if there is no early exit on Stage $K + 1 - i$, then this microbatch only need to go through the forward pass up to the last stage (among the first $K + 1 - i$ stages) that has at least one early exit.

Details about Part 2. We can calculate the maximum number of backward stages for each inserted microbatch, while ensuring that no overhead to training time per iteration occurs. Notice that for the i -th microbatch, the remaining bubble size after its forward computation at the last stage is $(p-1)b - f - (i-1)(f+b) = pb - i(f+b)$. Dividing this value by b gives the number of backward stages $\lfloor (pb - i(f+b))/b \rfloor = \lfloor p - i(f/b + 1) \rfloor$.

Some remarks. (1) There are some limitations to the proposed approach. For example, it requires that there is no tied/shared model parameter across pipeline stages; otherwise the gradients from partial forward/backward passes might (in theory) be harmful rather than beneficial for training the model. Another concern is that inserting microbatches into Part 1 of the explicit bubbles can cause additional overhead of activation memory in early stages. (2) While Part 1 of this approach requires the existence of early exits, Part 2 is actually applicable to training standard models without early exits as well. (3) One might raise concerns about the inefficiency of data usage, as some microbatches only undergo partial forward/backward passes. In general, this is not an issue for LLM pre-training, since training data is usually abundant, and the complete training process might not even go through one epoch of the data.

A different perspective. The actual implementation of this method in EE-LLM takes a different perspective. Instead of inserting additional microbatches into the original schedule, we keep the number of microbatches per training iteration unchanged, and do the following: (1) we replace the full forward/backward

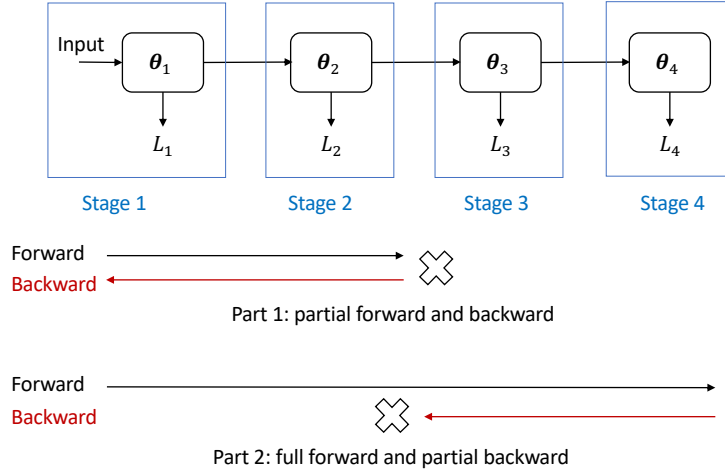


Figure 11: An illustration of the partial forward/backward passes when filling pipeline bubbles with additional microbatches.

computation of a few microbatches with partial forward/backward computation, which can be placed in the bubble between the warm-up and steady phases; (2) we truncate the backward computation of the last few microbatches. These two steps correspond exactly to Parts 1 and 2 introduced earlier, and the visualization in Figure 5(b) remains valid. Such an implementation reduces the training time per iteration, at the cost of lower data utilization.

B.2 Analysis

We argue that such partial forward/backward computation offers useful gradient information for training, under the assumption that there is no tied model parameter across pipeline stages. For a theoretical justification, let us take the perspective of stochastic optimization, and assume that each microbatch is sampled independently from some data distribution.

Claim 1 (Informal). *Under the above assumptions, the accumulated gradient of one training iteration, with extra updates from additional microbatches inserted into Part 2, remains (after some appropriate entrywise scaling) an unbiased estimate, but with reduced variance, of the gradient for the targeted population risk. A similar claim holds true for Part 1 as well, except for certain extreme (and unlikely) situations where gradients of different early/final losses have strong negative correlation.*

In the remaining of this section, we provide an informal proof for this claim, in a concrete example with four pipeline stages and one additional microbatch inserted into either Part 1 or Part 2; a visualization can be found in Figure 11. Recall that the training objective is defined as $\mathcal{L} = \sum_{i \in [4]} \mathcal{L}_i$, where each \mathcal{L}_i is a weighted sum of all losses on Stage i . We denote the model parameters as $\theta = [\theta_1, \theta_2, \theta_3, \theta_4]$, with correspondence to how the model is partitioned into four pipeline stages. One key observation that will be useful is that $\partial \mathcal{L}_i / \partial \theta_j = \mathbf{0}$ for any $1 \leq i < j \leq 4$, due to the sequential nature of the model.

Analysis of Part 2. We start with analysis for Part 2, which is slightly simpler. Suppose that an additional microbatch goes through the full forward pass, followed by a partial backward pass covering only the last two stages, namely θ_4 and θ_3 . Then, the gradient from this microbatch is

$$\text{gradient} = \left[\mathbf{0}, \mathbf{0}, \frac{\partial(\mathcal{L}_3 + \mathcal{L}_4)}{\partial \theta_3}, \frac{\partial(\mathcal{L}_3 + \mathcal{L}_4)}{\partial \theta_4} \right] = \left[\mathbf{0}, \mathbf{0}, \frac{\partial \mathcal{L}}{\partial \theta_3}, \frac{\partial \mathcal{L}}{\partial \theta_4} \right];$$

here, the first equality is due to the partial backward pass, and the second equality follows from the observation that $\partial \mathcal{L}_i / \partial \theta_j = \mathbf{0}$ for any $i < j$.

Now, suppose that a total of B microbatches was originally used for one training iteration, and we let $\mathcal{L}^{(k)}$ denote the loss of the k -th microbatch. Then, with the additional $(B + 1)$ -th microbatch inserted into Part 2 of the explicit bubbles, the accumulated gradient of one training iteration (normalized by $1/B$) becomes:

$$\begin{aligned} \text{accumulated gradient} &= \frac{1}{B} \left(\sum_{k \in [B]} \frac{\partial \mathcal{L}^{(k)}}{\partial \boldsymbol{\theta}} + \left[\mathbf{0}, \mathbf{0}, \frac{\partial \mathcal{L}^{(B+1)}}{\partial \boldsymbol{\theta}_3}, \frac{\partial \mathcal{L}^{(B+1)}}{\partial \boldsymbol{\theta}_4} \right] \right) \\ &= \left[\frac{1}{B} \sum_{k \in [B]} \frac{\partial \mathcal{L}^{(k)}}{\partial \boldsymbol{\theta}_1}, \frac{1}{B} \sum_{k \in [B]} \frac{\partial \mathcal{L}^{(k)}}{\partial \boldsymbol{\theta}_2}, \frac{1}{B} \sum_{k \in [B+1]} \frac{\partial \mathcal{L}^{(k)}}{\partial \boldsymbol{\theta}_3}, \frac{1}{B} \sum_{k \in [B+1]} \frac{\partial \mathcal{L}^{(k)}}{\partial \boldsymbol{\theta}_4} \right] \end{aligned}$$

Taking the expectation over the data distribution, we realize that the additional microbatch essentially scales up gradients for $\boldsymbol{\theta}_3$ and $\boldsymbol{\theta}_4$ by a factor of $(B + 1)/B$. Or, with a simple entrywise scaling on the gradients for $\boldsymbol{\theta}_3$ and $\boldsymbol{\theta}_4$ by a factor of $B/(B + 1)$, we recover an unbiased estimate of the gradient for the targeted population risk, with reduced variance:

$$\text{accumulated gradient} = \left[\frac{1}{B} \sum_{k \in [B]} \frac{\partial \mathcal{L}^{(k)}}{\partial \boldsymbol{\theta}_1}, \frac{1}{B} \sum_{k \in [B]} \frac{\partial \mathcal{L}^{(k)}}{\partial \boldsymbol{\theta}_2}, \frac{1}{B+1} \sum_{k \in [B+1]} \frac{\partial \mathcal{L}^{(k)}}{\partial \boldsymbol{\theta}_3}, \frac{1}{B+1} \sum_{k \in [B+1]} \frac{\partial \mathcal{L}^{(k)}}{\partial \boldsymbol{\theta}_4} \right].$$

Analysis of Part 1. Suppose that an additional microbatch goes through the forward and backward computation only for the first two stages, corresponding to model parameters $\boldsymbol{\theta}_1$ and $\boldsymbol{\theta}_2$. Then, the gradient from this microbatch is

$$\text{gradient} = \left[\frac{\partial(\mathcal{L}_1 + \mathcal{L}_2)}{\partial \boldsymbol{\theta}_1}, \frac{\partial(\mathcal{L}_1 + \mathcal{L}_2)}{\partial \boldsymbol{\theta}_2}, \mathbf{0}, \mathbf{0} \right] = \frac{\partial(\mathcal{L}_1 + \mathcal{L}_2)}{\partial \boldsymbol{\theta}};$$

here, the first equality is due to the partial forward and backward passes, and the second equality follows again from the observation that $\partial \mathcal{L}_i / \partial \boldsymbol{\theta}_j = \mathbf{0}$ for any $i < j$.

Now, suppose that a total of B microbatches was originally used for one training iteration. We denote the loss of the k -th microbatch as $\mathcal{L}^{(k)} = \sum_{i \in [4]} \mathcal{L}_i^{(k)}$. Then, with the additional $(B + 1)$ -th microbatch inserted into Part 1 of the explicit bubbles, the accumulated gradient of one training iteration (normalized by $1/B$) becomes:

$$\begin{aligned} \text{accumulated gradient} &= \frac{1}{B} \left(\sum_{k \in [B]} \frac{\partial \mathcal{L}^{(k)}}{\partial \boldsymbol{\theta}} + \frac{\partial(\mathcal{L}_1^{(B+1)} + \mathcal{L}_2^{(B+1)})}{\partial \boldsymbol{\theta}} \right) \\ &= \frac{1}{B} \left(\sum_{k \in [B]} \frac{\partial(\mathcal{L}_1^{(k)} + \mathcal{L}_2^{(k)} + \mathcal{L}_3^{(k)} + \mathcal{L}_4^{(k)})}{\partial \boldsymbol{\theta}} + \frac{\partial(\mathcal{L}_1^{(B+1)} + \mathcal{L}_2^{(B+1)})}{\partial \boldsymbol{\theta}} \right) \\ &= \frac{1}{B} \left(\sum_{k \in [B+1]} \frac{\partial(\mathcal{L}_1^{(k)} + \mathcal{L}_2^{(k)})}{\partial \boldsymbol{\theta}} + \sum_{k \in [B]} \frac{\partial(\mathcal{L}_3^{(k)} + \mathcal{L}_4^{(k)})}{\partial \boldsymbol{\theta}} \right). \end{aligned}$$

Taking the expectation over the data distribution, we see that the additional microbatch essentially scales up the weights of \mathcal{L}_1 and \mathcal{L}_2 in the gradient by a factor of $(B + 1)/B$. Or, if the weights of \mathcal{L}_1 and \mathcal{L}_2 are manually scaled by a factor of $B/(B + 1)$ during training, then we recover an unbiased gradient estimate for the original risk $\mathcal{L} = \sum_{i \in [4]} \mathcal{L}_i$:

$$\text{accumulated gradient} = \frac{1}{B+1} \sum_{k \in [B+1]} \frac{\partial(\mathcal{L}_1^{(k)} + \mathcal{L}_2^{(k)})}{\partial \boldsymbol{\theta}} + \frac{1}{B} \sum_{k \in [B]} \frac{\partial(\mathcal{L}_3^{(k)} + \mathcal{L}_4^{(k)})}{\partial \boldsymbol{\theta}}$$

We claim that this leads to reduced gradient variance, *unless* gradients of early and later losses have strong negative correlation. In the formal analysis of variance below, we consider scalars for notational simplicity, though it can be easily generalized to vectors or tensors by replacing scalar multiplication with inner product.

Proposition 2. Consider two distributions \mathcal{A} and \mathcal{B} with means a^* and b^* , respectively. Let a_1, \dots, a_N, a_{N+1} be independent and identically distributed (i.i.d.) samples of \mathcal{A} , and b_1, \dots, b_N be i.i.d. samples of \mathcal{B} , but for each i , a_i can be correlated with b_i . Consider two estimates of $a^* + b^*$, defined as follows:

$$\hat{e} := \hat{a}_N + \hat{b}_N, \quad \hat{e}_+ := \hat{a}_{N+1} + \hat{b}_N, \quad \text{where}$$

$$\hat{a}_k := \frac{1}{k} \sum_{i \in [k]} a_i, \quad \hat{b}_k := \frac{1}{k} \sum_{i \in [k]} b_i, \quad k \in \{N, N+1\}.$$

Then it holds that

$$\mathbb{E}[\hat{e}] = \mathbb{E}[\hat{e}_+] = a^* + b^*, \quad \text{var}(\hat{e}) - \text{var}(\hat{e}_+) = \frac{1}{N(N+1)} \text{var}(a_1) + \frac{2}{N(N+1)} \text{cov}(a_1, b_1).$$

In this proposition, \hat{a}_N, \hat{a}_{N+1} and \hat{b}_N correspond to $\frac{1}{B} \sum_{k \in [B]} \frac{\partial(\mathcal{L}_1^{(k)} + \mathcal{L}_2^{(k)})}{\partial \theta}$, $\frac{1}{B+1} \sum_{k \in [B+1]} \frac{\partial(\mathcal{L}_1^{(k)} + \mathcal{L}_2^{(k)})}{\partial \theta}$ and $\frac{1}{B} \sum_{k \in [B]} \frac{\partial(\mathcal{L}_3^{(k)} + \mathcal{L}_4^{(k)})}{\partial \theta}$ in our previous analysis of accumulated gradients, respectively. Hence our claim on gradient variance follows immediately from the conclusion of this proposition.

Proof of Proposition 2. First, unbiasedness is obvious. As for variance, we have the following elementary calculation:

$$\begin{aligned} \text{var}(\hat{e}) &= \mathbb{E}[(\hat{a}_N + \hat{b}_N - a^* - b^*)^2] = \mathbb{E}[(\hat{a}_N - a^*)^2] + \mathbb{E}[(\hat{b}_N - b^*)^2] + 2\mathbb{E}[(\hat{a}_N - a^*)(\hat{b}_N - b^*)], \\ \text{var}(\hat{e}_+) &= \mathbb{E}[(\hat{a}_{N+1} + \hat{b}_N - a^* - b^*)^2] = \mathbb{E}[(\hat{a}_{N+1} - a^*)^2] + \mathbb{E}[(\hat{b}_N - b^*)^2] + 2\mathbb{E}[(\hat{a}_{N+1} - a^*)(\hat{b}_N - b^*)]. \end{aligned}$$

Moreover,

$$\mathbb{E}[(\hat{a}_N - a^*)^2] = \frac{1}{N} \text{var}(a_1), \quad \mathbb{E}[(\hat{a}_{N+1} - a^*)^2] = \frac{1}{N+1} \text{var}(a_1),$$

and

$$\begin{aligned} \mathbb{E}[(\hat{a}_N - a^*)(\hat{b}_N - b^*)] &= \frac{1}{N^2} \sum_{i \in [N]} \mathbb{E}[(a_i - a^*)(b_i - b^*)] = \frac{1}{N} \text{cov}(a_1, b_1), \\ \mathbb{E}[(\hat{a}_{N+1} - a^*)(\hat{b}_N - b^*)] &= \frac{1}{N(N+1)} \sum_{i \in [N]} \mathbb{E}[(a_i - a^*)(b_i - b^*)] = \frac{1}{N+1} \text{cov}(a_1, b_1). \end{aligned}$$

Putting things together,

$$\begin{aligned} \text{var}(\hat{e}) - \text{var}(\hat{e}_+) &= \mathbb{E}[(\hat{a}_N - a^*)^2] - \mathbb{E}[(\hat{a}_{N+1} - a^*)^2] \\ &\quad + 2 \left(\mathbb{E}[(\hat{a}_N - a^*)(\hat{b}_N - b^*)] - \mathbb{E}[(\hat{a}_{N+1} - a^*)(\hat{b}_N - b^*)] \right) \\ &= \frac{1}{N(N+1)} \text{var}(a_1) + \frac{2}{N(N+1)} \text{cov}(a_1, b_1), \end{aligned}$$

which concludes our proof. □

References

- [1] Anonymous. A simple romance between multi-exit vision transformer and token reduction. In *Submitted to The Twelfth International Conference on Learning Representations, 2023*. under review.
- [2] Jimmy Ba, Jamie Ryan Kiros, and Geoffrey E. Hinton. Layer normalization. *ArXiv*, abs/1607.06450, 2016.
- [3] Sangmin Bae, Jongwoo Ko, Hwanjun Song, and Se-Young Yun. Fast and robust early-exiting framework for autoregressive language models with synchronized parallel decoding. *ArXiv*, abs/2310.05424, 2023.

- [4] Dzmitry Bahdanau, Kyunghyun Cho, and Yoshua Bengio. Neural machine translation by jointly learning to align and translate. In *ICLR*, 2015.
- [5] Emmanuel Bengio, Pierre-Luc Bacon, Joelle Pineau, and Doina Precup. Conditional computation in neural networks for faster models. *ArXiv*, abs/1511.06297, 2015.
- [6] Yoshua Bengio, Nicholas Léonard, and Aaron C. Courville. Estimating or propagating gradients through stochastic neurons for conditional computation. *ArXiv*, abs/1308.3432, 2013.
- [7] Rishi Bommasani, Drew A. Hudson, Ehsan Adeli, Russ Altman, Simran Arora, Sydney von Arx, Michael S. Bernstein, Jeannette Bohg, Antoine Bosselut, Emma Brunskill, Erik Brynjolfsson, S. Buch, Dallas Card, Rodrigo Castellon, Niladri S. Chatterji, Annie S. Chen, Kathleen A. Creel, Jared Davis, Dora Demszky, Chris Donahue, Moussa Doumbouya, Esin Durmus, Stefano Ermon, John Etchemendy, Kawin Ethayarajh, Li Fei-Fei, Chelsea Finn, Trevor Gale, Lauren Gillespie, Karan Goel, Noah D. Goodman, Shelby Grossman, Neel Guha, Tatsunori Hashimoto, Peter Henderson, John Hewitt, Daniel E. Ho, Jenny Hong, Kyle Hsu, Jing Huang, Thomas F. Icard, Saahil Jain, Dan Jurafsky, Pratyusha Kalluri, Siddharth Karamcheti, Geoff Keeling, Fereshte Khani, O. Khattab, Pang Wei Koh, Mark S. Krass, Ranjay Krishna, Rohith Kudithipudi, Ananya Kumar, Faisal Ladhak, Mina Lee, Tony Lee, Jure Leskovec, Isabelle Levent, Xiang Lisa Li, Xuechen Li, Tengyu Ma, Ali Malik, Christopher D. Manning, Suvir Mirchandani, Eric Mitchell, Zanele Munyikwa, Suraj Nair, Avanika Narayan, Deepak Narayanan, Benjamin Newman, Allen Nie, Juan Carlos Niebles, Hamed Nilforoshan, J. F. Nyarko, Giray Ogut, Laurel J. Orr, Isabel Papadimitriou, Joon Sung Park, Chris Piech, Eva Portelance, Christopher Potts, Aditi Raghunathan, Robert Reich, Hongyu Ren, Frieda Rong, Yusuf H. Roohani, Camilo Ruiz, Jack Ryan, Christopher R’e, Dorsa Sadigh, Shiori Sagawa, Keshav Santhanam, Andy Shih, Krishna Parasuram Srinivasan, Alex Tamkin, Rohan Taori, Armin W. Thomas, Florian Tramèr, Rose E. Wang, William Wang, Bohan Wu, Jiajun Wu, Yuhuai Wu, Sang Michael Xie, Michihiro Yasunaga, Jiaxuan You, Matei A. Zaharia, Michael Zhang, Tianyi Zhang, Xikun Zhang, Yuhui Zhang, Lucia Zheng, Kaitlyn Zhou, and Percy Liang. On the opportunities and risks of foundation models. *ArXiv*, abs/2108.07258, 2021.
- [8] Tom B. Brown, Benjamin Mann, Nick Ryder, Melanie Subbiah, Jared Kaplan, Prafulla Dhariwal, Arvind Neelakantan, Pranav Shyam, Girish Sastry, Amanda Askell, Sandhini Agarwal, Ariel Herbert-Voss, Gretchen Krueger, Tom Henighan, Rewon Child, Aditya Ramesh, Daniel M. Ziegler, Jeffrey Wu, Clemens Winter, Christopher Hesse, Mark Chen, Eric Sigler, Mateusz Litwin, Scott Gray, Benjamin Chess, Jack Clark, Christopher Berner, Sam McCandlish, Alec Radford, Ilya Sutskever, and Dario Amodei. Language models are few-shot learners. In *NeurIPS*, 2020.
- [9] Daoyuan Chen, Yilun Huang, Zhijian Ma, Heseng Chen, Xuchen Pan, Ce Ge, Dawei Gao, Yuexiang Xie, Zhaoyang Liu, Jinyang Gao, Yaliang Li, Bolin Ding, and Jingren Zhou. Data-juicer: A one-stop data processing system for large language models. *ArXiv*, abs/2309.02033, 2023.
- [10] Tianqi Chen, Bing Xu, Chiyuan Zhang, and Carlos Guestrin. Training deep nets with sublinear memory cost. *ArXiv*, abs/1604.06174, 2016.
- [11] Aakanksha Chowdhery, Sharan Narang, Jacob Devlin, Maarten Bosma, Gaurav Mishra, Adam Roberts, Paul Barham, Hyung Won Chung, Charles Sutton, Sebastian Gehrmann, Parker Schuh, Kensen Shi, Sasha Tsvyashchenko, Joshua Maynez, Abhishek Rao, Parker Barnes, Yi Tay, Noam Shazeer, Vinodkumar Prabhakaran, Emily Reif, Nan Du, Ben Hutchinson, Reiner Pope, James Bradbury, Jacob Austin, Michael Isard, Guy Gur-Ari, Pengcheng Yin, Toju Duke, Anselm Levskaya, Sanjay Ghemawat, Sunipa Dev, Henryk Michalewski, Xavier Garcia, Vedant Misra, Kevin Robinson, Liam Fedus, Denny Zhou, Daphne Ippolito, David Luan, Hyeontaek Lim, Barret Zoph, Alexander Spiridonov, Ryan Sepassi, David Dohan, Shivani Agrawal, Mark Omernick, Andrew M. Dai, Thanumalayan Sankaranarayanan Pillai, Marie Pellat, Aitor Lewkowycz, Erica Moreira, Rewon Child, Oleksandr Polozov, Katherine Lee, Zongwei Zhou, Xuezhi Wang, Brennan Saeta, Mark Diaz, Orhan Firat, Michele Catasta, Jason Wei, Kathy Meier-Hellstern, Douglas Eck, Jeff Dean, Slav Petrov, and Noah Fiedel. Palm: Scaling language modeling with pathways. *J. Mach. Learn. Res.*, 24:240:1–240:113, 2023.
- [12] Christopher Clark, Kenton Lee, Ming-Wei Chang, Tom Kwiatkowski, Michael Collins, and Kristina Toutanova. Boolq: Exploring the surprising difficulty of natural yes/no questions. In *NAACL*, 2019.

- [13] Luciano Del Corro, Allison Del Giorno, Sahaj Agarwal, Ting Yu, Ahmed Hassan Awadallah, and Subhabrata Mukherjee. Skipdecode: Autoregressive skip decoding with batching and caching for efficient llm inference. *ArXiv*, abs/2307.02628, 2023.
- [14] Yinwei Dai, Rui Pan, Anand Iyer, Kai Li, and Ravi Netravali. Apparate: Rethinking early exits to tame latency-throughput tensions in ml serving. *ArXiv*, abs/2312.05385, 2023.
- [15] Tri Dao, Daniel Y Fu, Stefano Ermon, Atri Rudra, and Christopher Re. Flashattention: Fast and memory-efficient exact attention with IO-awareness. In *NeurIPS*, 2022.
- [16] Jacob Devlin, Ming-Wei Chang, Kenton Lee, and Kristina Toutanova. Bert: Pre-training of deep bidirectional transformers for language understanding. In *North American Chapter of the Association for Computational Linguistics*, 2019.
- [17] Alexander Yom Din, Taelin Karidi, Leshem Choshen, and Mor Geva. Jump to conclusions: Short-cutting transformers with linear transformations. *ArXiv*, abs/2303.09435, 2023.
- [18] Rahul Duggal, Scott Freitas, Sunny Dhamnani, Duen Horng Chau, and Jimeng Sun. Elf: An early-exiting framework for long-tailed classification. *ArXiv*, abs/2006.11979, 2020.
- [19] Maha Elbayad, Jiatao Gu, Edouard Grave, and Michael Auli. Depth-adaptive transformer. In *ICLR*, 2020.
- [20] Shiqing Fan, Yi Rong, Chen Meng, Zongyan Cao, Siyu Wang, Zhen Zheng, Chuan Wu, Guoping Long, Jun Yang, Lixue Xia, Lansong Diao, Xiaoyong Liu, and Wei Lin. DAPPLE: a pipelined data parallel approach for training large models. In *PPoPP*, pages 431–445, 2021.
- [21] William Fedus, Barret Zoph, and Noam M. Shazeer. Switch transformers: Scaling to trillion parameter models with simple and efficient sparsity. *J. Mach. Learn. Res.*, 23:120:1–120:39, 2021.
- [22] Ariel Gera, Roni Friedman, Ofir Arviv, Chulaka Gunasekara, Benjamin Sznajder, Noam Slonim, and Eyal Shnarch. The benefits of bad advice: Autocontrastive decoding across model layers. In *ACL*, 2023.
- [23] Alex Graves. Adaptive computation time for recurrent neural networks. *ArXiv*, abs/1603.08983, 2016.
- [24] Yizeng Han, Gao Huang, Shiji Song, Le Yang, Honghui Wang, and Yulin Wang. Dynamic neural networks: A survey. *IEEE Trans. Pattern Anal. Mach. Intell.*, 44(11):7436–7456, 2022.
- [25] Lu Hou, Zhiqi Huang, Lifeng Shang, Xin Jiang, Xiao Chen, and Qun Liu. Dynabert: Dynamic BERT with adaptive width and depth. In *NeurIPS*, 2020.
- [26] Boren Hu, Yun Zhu, Jiacheng Li, and Siliang Tang. Smartbert: A promotion of dynamic early exiting mechanism for accelerating bert inference. In *IJCAI*, 2023.
- [27] Gao Huang, Danlu Chen, Tianhong Li, Felix Wu, Laurens van der Maaten, and Kilian Q. Weinberger. Multi-scale dense networks for resource efficient image classification. In *ICLR*, 2018.
- [28] Yanping Huang, Youlong Cheng, Ankur Bapna, Orhan Firat, Dehao Chen, Mia Xu Chen, HyoukJoong Lee, Jiquan Ngiam, Quoc V. Le, Yonghui Wu, and Zhifeng Chen. Gpipe: Efficient training of giant neural networks using pipeline parallelism. In *NeurIPS*, pages 103–112, 2019.
- [29] Fatih Ilhan, Gong Su, and Ling Liu. Scalefl: Resource-adaptive federated learning with heterogeneous clients. In *CVPR*, pages 24532–24541, 2023.
- [30] Robert A. Jacobs, Michael I. Jordan, Steven J. Nowlan, and Geoffrey E. Hinton. Adaptive mixtures of local experts. *Neural Computation*, 3:79–87, 1991.
- [31] Yigitcan Kaya, Sanghyun Hong, and Tudor Dumitras. Shallow-deep networks: Understanding and mitigating network overthinking. In *ICML*, volume 97, pages 3301–3310, 2019.

- [32] Sehoon Kim, Coleman Hooper, Thanakul Wattanawong, Minwoo Kang, Ruohan Yan, Hasan Gen̄, Grace Dinh, Qijing Huang, Kurt Keutzer, Michael W. Mahoney, Yakun Sophia Shao, and Amir Gholami. Full stack optimization of transformer inference: a survey. *ArXiv*, abs/2302.14017, 2023.
- [33] Sehoon Kim, Karttikeya Mangalam, Suhong Moon, Jitendra Malik, Michael W. Mahoney, Amir Gholami, and Kurt Keutzer. Speculative decoding with big little decoder. In *NeurIPS*, 2023.
- [34] Yoon Kim, Carl Denton, Luong Hoang, and Alexander M. Rush. Structured attention networks. In *ICLR*, 2017.
- [35] Diederik P. Kingma and Jimmy Ba. Adam: A method for stochastic optimization. In *ICLR*, 2014.
- [36] Vijay Anand Korthikanti, Jared Casper, Sangkug Lym, Lawrence C. McAfee, Michael Andersch, Mohammad Shoeybi, and Bryan Catanzaro. Reducing activation recomputation in large transformer models. *ArXiv*, abs/2205.05198, 2022.
- [37] Anna Langedijk, Hosein Mohebbi, Gabriele Sarti, Willem H. Zuidema, and Jaap Jumelet. Decoderlens: Layerwise interpretation of encoder-decoder transformers. *ArXiv*, abs/2310.03686, 2023.
- [38] Stefanos Laskaridis, Alexandros Kouris, and Nicholas Donald Lane. Adaptive inference through early-exit networks: Design, challenges and directions. In *International Workshop on Embedded and Mobile Deep Learning*, 2021.
- [39] Chen-Yu Lee, Saining Xie, Patrick W. Gallagher, Zhengyou Zhang, and Zhuowen Tu. Deeply-supervised nets. In *AISTATS*, 2014.
- [40] Yaniv Leviathan, Matan Kalman, and Yossi Matias. Fast inference from transformers via speculative decoding. In *ICML*, 2022.
- [41] Shigang Li and Torsten Hoefer. Chimera: efficiently training large-scale neural networks with bidirectional pipelines. In *SC*, page 27, 2021.
- [42] Xiaonan Li, Yunfan Shao, Tianxiang Sun, Hang Yan, Xipeng Qiu, and Xuanjing Huang. Accelerating bert inference for sequence labeling via early-exit. In *ACL*, 2021.
- [43] Percy Liang, Rishi Bommasani, Tony Lee, Dimitris Tsipras, Dilara Soylu, Michihiro Yasunaga, Yian Zhang, Deepak Narayanan, Yuhuai Wu, Ananya Kumar, Benjamin Newman, Binhang Yuan, Bobby Yan, Ce Zhang, Christian Cosgrove, Christopher D. Manning, Christopher R’e, Diana Acosta-Navas, Drew A. Hudson, E. Zelikman, Esin Durmus, Faisal Ladhak, Frieda Rong, Hongyu Ren, Huaxiu Yao, Jue Wang, Keshav Santhanam, Laurel J. Orr, Lucia Zheng, Mert Yuksekgonul, Mirac Suzgun, Nathan S. Kim, Neel Guha, Niladri S. Chatterji, Omar Khattab, Peter Henderson, Qian Huang, Ryan Chi, Sang Michael Xie, Shibani Santurkar, Surya Ganguli, Tatsunori Hashimoto, Thomas F. Icard, Tianyi Zhang, Vishrav Chaudhary, William Wang, Xuechen Li, Yifan Mai, Yuhui Zhang, and Yuta Koreeda. Holistic evaluation of language models. *Annals of the New York Academy of Sciences*, 1525:140 – 146, 2023.
- [44] Stephanie Lin, Jacob Hilton, and Owain Evans. Truthfulqa: Measuring how models mimic human falsehoods. In *ACL*, pages 3214–3252, 2022.
- [45] Weijie Liu, Peng Zhou, Zhiruo Wang, Zhe Zhao, Haotang Deng, and Qi Ju. Fastbert: a self-distilling BERT with adaptive inference time. In *ACL*, pages 6035–6044, 2020.
- [46] Shashi Narayan, Shay B. Cohen, and Mirella Lapata. Don’t give me the details, just the summary! topic-aware convolutional neural networks for extreme summarization. In *EMNLP*, pages 1797–1807, 2018.
- [47] Deepak Narayanan, Aaron Harlap, Amar Phanishayee, Vivek Seshadri, Nikhil R. Devanur, Gregory R. Ganger, Phillip B. Gibbons, and Matei Zaharia. Pipedream: generalized pipeline parallelism for DNN training. In *SOSP*, pages 1–15, 2019.

- [48] Deepak Narayanan, Amar Phanishayee, Kaiyu Shi, Xie Chen, and Matei Zaharia. Memory-efficient pipeline-parallel DNN training. In *ICML*, volume 139, pages 7937–7947, 2021.
- [49] Deepak Narayanan, Mohammad Shoeybi, Jared Casper, Patrick LeGresley, Mostofa Patwary, Vijay Korthikanti, Dmitri Vainbrand, Prethvi Kashinkunti, Julie Bernauer, Bryan Catanzaro, Amar Phanishayee, and Matei Zaharia. Efficient large-scale language model training on GPU clusters using megatron-lm. In *SC*, page 58, 2021.
- [50] OpenAI. Gpt-4 technical report. *ArXiv*, abs/2303.08774, 2023.
- [51] Kazuki Osawa, Shigang Li, and Torsten Hoefer. Pipefisher: Efficient training of large language models using pipelining and fisher information matrices. In *MLSys*, 2023.
- [52] Ankur Parikh, Oscar Täckström, Dipanjan Das, and Jakob Uszkoreit. A decomposable attention model for natural language inference. In *EMNLP*, pages 2249–2255, 2016.
- [53] Reiner Pope, Sholto Douglas, Aakanksha Chowdhery, Jacob Devlin, James Bradbury, Anselm Levskaya, Jonathan Heek, Kefan Xiao, Shivani Agrawal, and Jeff Dean. Efficiently scaling transformer inference. *ArXiv*, abs/2211.05102, 2022.
- [54] Ofir Press and Lior Wolf. Using the output embedding to improve language models. In *EACL*, pages 157–163, 2017.
- [55] Alec Radford, Karthik Narasimhan, Tim Salimans, and Ilya Sutskever. Improving language understanding by generative pre-training, 2018.
- [56] Alec Radford, Jeff Wu, Rewon Child, David Luan, Dario Amodei, and Ilya Sutskever. Language models are unsupervised multitask learners, 2019.
- [57] Samyam Rajbhandari, Jeff Rasley, Olatunji Ruwase, and Yuxiong He. Zero: Memory optimizations toward training trillion parameter models. In *SC*, 2019.
- [58] Jeff Rasley, Samyam Rajbhandari, Olatunji Ruwase, and Yuxiong He. Deepspeed: System optimizations enable training deep learning models with over 100 billion parameters. In *KDD*, pages 3505–3506, 2020.
- [59] Andrea Santilli, Silvio Severino, Emilian Postolache, Valentino Maiorca, Michele Mancusi, Riccardo Marin, and Emanuele Rodolà. Accelerating transformer inference for translation via parallel decoding. In *ACL*, 2023.
- [60] Simone Scardapane, Michele Scarpiniti, Enzo Baccarelli, and Aurelio Uncini. Why should we add early exits to neural networks? *Cognitive Computation*, 12:954 – 966, 2020.
- [61] Tal Schuster, Adam Fisch, Jai Gupta, Mostafa Dehghani, Dara Bahri, Vinh Tran, Yi Tay, and Donald Metzler. Confident adaptive language modeling. In *NeurIPS*, 2022.
- [62] Tal Schuster, Adam Fisch, Tommi S. Jaakkola, and Regina Barzilay. Consistent accelerated inference via confident adaptive transformers. In *EMNLP*, pages 4962–4979, 2021.
- [63] Roy Schwartz, Gabriel Stanovsky, Swabha Swayamdipta, Jesse Dodge, and Noah A. Smith. The right tool for the job: Matching model and instance complexities. In *ACL*, pages 6640–6651, 2020.
- [64] Abigail See, Peter J. Liu, and Christopher D. Manning. Get to the point: Summarization with pointer-generator networks. In *ACL*, pages 1073–1083, 2017.
- [65] Noam Shazeer, Youlong Cheng, Niki Parmar, Dustin Tran, Ashish Vaswani, Penporn Koanantakool, Peter Hawkins, HyoukJoong Lee, Mingsheng Hong, Cliff Young, Ryan Sepassi, and Blake Hechtman. Mesh-tensorflow: Deep learning for supercomputers. In *NIPS*, pages 10435–10444, 2018.
- [66] Noam M. Shazeer, Azalia Mirhoseini, Krzysztof Maziarz, Andy Davis, Quoc V. Le, Geoffrey E. Hinton, and Jeff Dean. Outrageously large neural networks: The sparsely-gated mixture-of-experts layer. In *ICLR*, 2017.

- [67] Mohammad Shoeybi, Mostofa Patwary, Raul Puri, Patrick LeGresley, Jared Casper, and Bryan Catanzaro. Megatron-lm: Training multi-billion parameter language models using model parallelism. *ArXiv*, abs/1909.08053, 2019.
- [68] Shaden Smith, Mostofa Patwary, Brandon Norick, Patrick LeGresley, Samyam Rajbhandari, Jared Casper, Zhun Liu, Shrimai Prabhunoye, George Zerveas, Vijay Anand Korthikanti, Elton Zhang, Rewon Child, Reza Yazdani Aminabadi, Julie Bernauer, Xia Song, Mohammad Shoeybi, Yuxiong He, Michael Houston, Saurabh Tiwary, and Bryan Catanzaro. Using deepspeed and megatron to train megatron-turing nlg 530b, a large-scale generative language model. *ArXiv*, abs/2201.11990, 2022.
- [69] Christian Szegedy, Wei Liu, Yangqing Jia, Pierre Sermanet, Scott E. Reed, Dragomir Anguelov, D. Erhan, Vincent Vanhoucke, and Andrew Rabinovich. Going deeper with convolutions. In *CVPR*, 2015.
- [70] Peng Tang, Pengkai Zhu, Tian Li, Srikar Appalaraju, Vijay Mahadevan, and R. Manmatha. Deed: Dynamic early exit on decoder for accelerating encoder-decoder transformer models. *ArXiv*, abs/2311.08623, 2023.
- [71] Yi Tay, Mostafa Dehghani, Dara Bahri, and Donald Metzler. Efficient transformers: A survey. *ACM Comput. Surv.*, 55(6), 2022.
- [72] InternLM Team. Internlm: A multilingual language model with progressively enhanced capabilities. <https://github.com/InternLM/InternLM>, 2023.
- [73] Surat Teerapittayanon, Bradley McDanel, and H. T. Kung. Branchynet: Fast inference via early exiting from deep neural networks. In *ICPR*, pages 2464–2469, 2016.
- [74] Hugo Touvron, Thibaut Lavril, Gautier Izacard, Xavier Martinet, Marie-Anne Lachaux, Timothée Lacroix, Baptiste Rozière, Naman Goyal, Eric Hambro, Faisal Azhar, Aurelien Rodriguez, Armand Joulin, Edouard Grave, and Guillaume Lample. Llama: Open and efficient foundation language models. *ArXiv*, abs/2302.13971, 2023.
- [75] Hugo Touvron, Louis Martin, Kevin R. Stone, Peter Albert, Amjad Almahairi, Yasmine Babaei, Nikolay Bashlykov, Soumya Batra, Prajjwal Bhargava, Shruiti Bhosale, Daniel M. Bikel, Lukas Blecher, Cristian Cantón Ferrer, Moya Chen, Guillem Cucurull, David Esiobu, Jude Fernandes, Jeremy Fu, Wenyin Fu, Brian Fuller, Cynthia Gao, Vedanuj Goswami, Naman Goyal, Anthony S. Hartshorn, Saghar Hosseini, Rui Hou, Hakan Inan, Marcin Kardas, Viktor Kerkez, Madian Khabsa, Isabel M. Kloumann, A. V. Korenev, Punit Singh Koura, Marie-Anne Lachaux, Thibaut Lavril, Jenya Lee, Diana Liskovich, Yinghai Lu, Yuning Mao, Xavier Martinet, Todor Mihaylov, Pushkar Mishra, Igor Molybog, Yixin Nie, Andrew Poulton, Jeremy Reizenstein, Rashi Rungta, Kalyan Saladi, Alan Schelten, Ruan Silva, Eric Michael Smith, R. Subramanian, Xia Tan, Binh Tang, Ross Taylor, Adina Williams, Jian Xiang Kuan, Puxin Xu, Zhengxu Yan, Iliyan Zarov, Yuchen Zhang, Angela Fan, Melanie Kambadur, Sharan Narang, Aurelien Rodriguez, Robert Stojnic, Sergey Edunov, and Thomas Scialom. Llama 2: Open foundation and fine-tuned chat models. *ArXiv*, abs/2307.09288, 2023.
- [76] Neeraj Varshney, Agneet Chatterjee, Mihir Parmar, and Chitta Baral. Accelerating llama inference by enabling intermediate layer decoding via instruction tuning with lite. *ArXiv*, abs/2310.18581, 2023.
- [77] Ashish Vaswani, Noam Shazeer, Niki Parmar, Jakob Uszkoreit, Llion Jones, Aidan N. Gomez, Lukasz Kaiser, and Illia Polosukhin. Attention is all you need. In *NeurIPS*, pages 5998–6008, 2017.
- [78] Haoyu Wang, Yaqing Wang, Tianci Liu, Tuo Zhao, and Jing Gao. Hadskip: Homotopic and adaptive layer skipping of pre-trained language models for efficient inference. In *Conference on Empirical Methods in Natural Language Processing*, 2023.
- [79] Jue Wang, Ke Chen, Gang Chen, Lidan Shou, and Julian McAuley. Skipbert: Efficient inference with shallow layer skipping. In *ACL*, 2022.

- [80] Guangxuan Xiao, Ji Lin, Mickael Seznec, Hao Wu, Julien Demouth, and Song Han. SmoothQuant: Accurate and efficient post-training quantization for large language models. In *ICML*, volume 202, pages 38087–38099, 2023.
- [81] Ji Xin, Raphael Tang, Jaejun Lee, Yaoliang Yu, and Jimmy Lin. Deebert: Dynamic early exiting for accelerating BERT inference. In *ACL*, pages 2246–2251, 2020.
- [82] Ji Xin, Raphael Tang, Yaoliang Yu, and Jimmy Lin. Berxit: Early exiting for BERT with better fine-tuning and extension to regression. In *EACL*, pages 91–104, 2021.
- [83] Canwen Xu and Julian McAuley. A survey on dynamic neural networks for natural language processing. In *EACL*, pages 2370–2381. Association for Computational Linguistics, 2023.
- [84] Fei Yang, Shuang Peng, Ning Sun, Fangyu Wang, Ke Tan, Fu Wu, Jiezhong Qiu, and Aimin Pan. Holmes: Towards distributed training across clusters with heterogeneous nic environment. *ArXiv*, abs/2312.03549, 2023.
- [85] Zhewei Yao, Reza Yazdani Aminabadi, Minjia Zhang, Xiaoxia Wu, Conglong Li, and Yuxiong He. Zeroquant: Efficient and affordable post-training quantization for large-scale transformers. In *NeurIPS*, 2022.
- [86] Binhang Yuan, Yongjun He, Jared Davis, Tianyi Zhang, Tri Dao, Beidi Chen, Percy Liang, Christopher Ré, and Ce Zhang. Decentralized training of foundation models in heterogeneous environments. In *NeurIPS*, 2022.
- [87] Dwen Zeng, Nan Du, Tao Wang, Yuanzhong Xu, Tao Lei, Zhifeng Chen, and Claire Cui. Learning to skip for language modeling. *ArXiv*, abs/2311.15436, 2023.
- [88] Biao Zhang and Rico Sennrich. Root mean square layer normalization. In *NeurIPS*, pages 12360–12371, 2019.
- [89] Susan Zhang, Stephen Roller, Naman Goyal, Mikel Artetxe, Moya Chen, Shuohui Chen, Christopher Dewan, Mona T. Diab, Xian Li, Xi Victoria Lin, Todor Mihaylov, Myle Ott, Sam Shleifer, Kurt Shuster, Daniel Simig, Punit Singh Koura, Anjali Sridhar, Tianlu Wang, and Luke Zettlemoyer. Opt: Open pre-trained transformer language models. *ArXiv*, abs/2205.01068, 2022.
- [90] Wayne Xin Zhao, Kun Zhou, Junyi Li, Tianyi Tang, Xiaolei Wang, Yupeng Hou, Yingqian Min, Beichen Zhang, Junjie Zhang, Zican Dong, Yifan Du, Chen Yang, Yushuo Chen, Z. Chen, Jinhao Jiang, Ruiyang Ren, Yifan Li, Xinyu Tang, Zikang Liu, Peiyu Liu, Jianyun Nie, and Ji rong Wen. A survey of large language models. *ArXiv*, abs/2303.18223, 2023.
- [91] Yao Zhao, Zhitian Xie, Chenyi Zhuang, and Jinjie Gu. Lookahead: An inference acceleration framework for large language model with lossless generation accuracy. *ArXiv*, abs/2312.12728, 2023.
- [92] Lianmin Zheng, Zhuohan Li, Hao Zhang, Yonghao Zhuang, Zhifeng Chen, Yanping Huang, Yida Wang, Yuanzhong Xu, Danyang Zhuo, Eric P. Xing, Joseph E. Gonzalez, and Ion Stoica. Alpa: Automating inter- and Intra-Operator parallelism for distributed deep learning. In *OSDI*, pages 559–578, 2022.
- [93] Zhengyi Zhong, Ji Wang, Weidong Bao, Jingxuan Zhou, Xiaomin Zhu, and Xiongtao Zhang. Semi-hfl: semi-supervised federated learning for heterogeneous devices. *Complex & Intelligent Systems*, 9:1995–2017, 2022.
- [94] Wangchunshu Zhou, Canwen Xu, Tao Ge, Julian J. McAuley, Ke Xu, and Furu Wei. BERT loses patience: Fast and robust inference with early exit. In *NeurIPS*, 2020.